Bioconvective MHD Micropolar nanofluid flow with nonlinear thermal radiation and Joule heating effects in a stratified medium

Thesis Submitted By:

HABIB UN NISA
(01-248172-004)

Supervised By

Prof. Dr. M. Ramzan

A dissertation submitted to the Department of Computer Science, Bahria University, Islamabad as a partial fulfilment of the requirements for the award of the degree of MS

Session (2017 - 2019

Bahria University
Discovering Knowledge

MS-13

Thesis Completion Certificate

Scholar's Name: **Habib Un Nisa** Registration No. **01-248172-004**

Programmed of Study: **MS (Mathematics)**

Thesis Title: **"Bioconvective MHD Micropolar nanofluid flow with nonlinear thermal radiation and joule heating effects in a stratified medium"**

It is to certify that the above student's thesis has been completed to my satisfaction and, to my belief, its standard is appropriate for submission for Evaluation. I have also conducted plagiarism test of this thesis using HEC prescribed software and found similarity index at 01 % that is within the permissible limit set by the HEC for the MS/MPhil degree thesis.

I have also found the thesis in a format recognized by the BU for the MS/MPhil thesis.

Principal Supervisor's Signature: _____ 20/06/2019

Date: 20/06/2019 **Name:** Dr. Muhammad Ramzan

Dedicated to

My beloved parents and respected teachers

whose prayers and support have always been a source of inspiration

and encouragement for me.

My caring and supporting father

have always given me care and love.

Acknowledgments

I am thankful to Almighty ALLAH Who has enabled me to learn and to achieve milestones towards my destination and His beloved Prophet Hazrat Muhammad (ﷺ) Who is forever a constant source of guidance, a source of knowledge and blessing for entire creation. His teachings show us a way to live with dignity, stand with honour and learn to be humble.

My acknowledgment is to my kind, diligent and highly zealous supervisor, Prof. Dr. M. Ramzan, who supported me with his cherished opinions and inspirational discussions. His valuable expertise, comments, suggestions and instructions are most welcome that greatly improved the clarity of this document. I am placing my earnest thanks to Prof. Dr. M. Ramzan. I am so grateful to work under the supervision of such a great person.

My gratitude is to my honorable professors who took me to the apex of my academia with their guidance. In particular, Dr. Rizwan ul haq and Dr. Jafar Hasnain who have always been supportive in all of my course work and kept encouraging me throughout the session in Bahria University, Islamabad Campus. They are the true teachers who have made Mathematics Department of BUIC, a real place of learning.

My intense recognition is to my mother, father and brother (for everything) who are always real pillars for my encouragement and showered their everlasting love, care and support throughout my life. Humble prayers, continuing support and encouragement of my family are as always highly appreciated.

As usual, so many friends have helped me that I cannot list them all. Hina Gul, Saima Riasat and Asma Liaquet were specially remained enormously helpful throughout the period of

my MS studies.

Consequently, My all plea is to Allah, the Almighty, the beneficent Whose blessings are always showered upon me via strengthening my wisdom and bestowed me with the knowledge of what he wants.

Habib Un Nisa
Bahria University Islamabad, Pakistan
May 2019

Bahria University
Discovering Knowledge

MS-14A

Author's Declaration

I, **Habib Un Nisa** hereby state that my MS thesis titled **"Bioconvective MHD Micropolar nanofluid flow with nonlinear thermal radiation and joule heating effects in a stratified medium"** is my own work and has not been submitted previously by me for taking any degree from this university **Bahria University Islamabad**
or anywhere else in the country/world.

At any time if my statement is found to be incorrect even after my Graduate the university has the right to withdraw/cancel my MS degree.

Name of scholar: **Habib Un Nisa**
Date: **20/06/2019**

Bahria University
Discovering Knowledge

MS-14B

Plagiarism Undertaking

I solemnly declare that research work presented in the thesis titled **"Bioconvective MHD Micropolar nanofluid flow with nonlinear thermal radiation and joule heating effects in a stratified medium"** is solely my research work with no significant contribution from any other person. Small contribution / help wherever taken has been duly acknowledged and that complete thesis has been written by me.

I understand the zero tolerance policy of the HEC and Bahria University towards plagiarism. Therefore I as an Author of the above titled thesis declare that no portion of my thesis has been plagiarized and any material used as reference is properly referred / cited.

I undertake that if I am found guilty of any formal plagiarism in the above titled thesis even after award of MS degree, the university reserves the right to withdraw / revoke my MS degree and that HEC and the University has the right to publish my name on the HEC / University website on which names of students are placed who submitted plagiarized thesis.

Student / Author's Sign: Habiba

Name of the Student: **Habib Un Nisa**

Abstract

In this proposal MHD flow of a micropolar nanofluid with bioconvection past a penetrable elongating sheet in attendance of nonlinear thermal radiation and stratification conditions will be studied. In addition, effects of thermal and concentration stratification boundary conditions will also be discussed. Boundary layer system of non-linear partial differential equations will be converted to ordinary differential equations with high non-linearity via suitable transformations. Renowned Homotopy Analysis method (HAM) will be engaged to find series solution of the problem. Graphs of pertinent parameters against temperature, velocity, and concentration distributions will also be a part of this study.

List of Figures

List of tables

Nomenclature

τ_{yx}	Shear force applied on the element of fluid
$\frac{du}{dy}$	Shear rate
η_1	Apparent viscosity
η	Similarity variable
k_2	Consistency index
σ	Electrical conductivity
Q_1	Heat added
c	Specific heat
m	Mass
ΔT	Change in temperature
T_1	Temperature of the solid surface
T_2	Temperature of surrounding fluid
A	Surface area
h	Heat transfer coefficient
k_1, k_3, k_4, k_5	Thermal conductivity
x_i	Coordinate at the boundary
c_p	Specific heat
τ_w	Wall shear stress
U_w	Velocity
b	Chemotaxis constant
ρ_f	Density of nanofluid

b_1	Body force
e	Specific internal energy
r	Thermal radiation
x, y	Coordinate axis
μ	Dynamic viscosity
ν	Kinematic viscosity
N	Micro-rotation or angular velocity
ρ	Density
j	Microinertia density
γ^*	Spin gradient viscosity
u, v	Velocity components
B_0	Applied magnetic field strength
E_0	Applied electric field
k^*	Mean absorption coefficient
h_f	Heat transfer coefficient
α	Slip parameter
α^*	Slip coefficient
v_w, f_w	Suction/injection velocity
T	Fluid temperature
T_∞	Ambient temperature
T_f	Convective fluid temperature
T_0	Fluid reference temperature
T_w	Wall temperature
K	Material parameter

M, M_1^2	Hartman number
E	Electric parameter
R	Radiation parameter
Ec	Eckert number
$\Pr$	Prandtl number
Lb	Bioconvection lewis number
Le	Lewis number
Ω	Microorganisms concentration difference parameter
Pe	Bio-convection Peclet number
Nt	Thermophoresis parameter
Nb	Brownian motion parameter
C	Concentration of fluid
C_∞	Ambient concentration
C_f	Convective fluid concentration
C_0	Reference concentration of nano particles
D_B	Brownian diffusion coefficient
D_T	Thermophoretic diffusion coefficient
D_m	Microorganism diffusion coefficient
W_c	Maximum cell swimming speed
n	Density motile of microorganisms
n_0	Reference concentration of microorganisms

n_{∞}	Ambient concentration of microorganisms
n_f	Surface concentration of microorganisms
S	Thermal stratification parameter
P	Concentration stratification parameter
Q	Motile density stratification parameter
C_{f_x}	Skin friction number
Nu_x	Nusselt number
Sh_x	Sherwood number
Nn_x	Local density number
Q_L	Heat transferred with unit thickness of a substance per unit time
q_w	Heat flux at wall
τ	Ratio of effective heat
τ^*	Cauchy stress tensor
q	Heat flux
k	Vortex velocity
σ^*	Stefan-Boltzmann constant
q_r	Radiative heat flux

Contents

Chapter 1

Introduction and Literature review

1.1 Introduction

Nanofluids have many advantages over other simple fluids due to their thermal efficiency. Nanofluids are liquid suspensions in which nanoparticles including metals, polymers, metaloxides, silica etc., are added to a base fluid such as water, ethylene glycol, oil etc. Nanoparticles are basically the nanometer sized solid particles having diameter less than 100nm. Nanofluids have higher heat transfer rates, greater viscosity, higher thermal conductivity and more stability than other fluids. These fluids possess a better wetting, spreading and dispersion properties over a solid surface. The use of nanofluids spread over a wide range of fields. Nanofluids serve as a coolant in heat transfer equipment like electronic cooling system, heat exchangers and radiators etc. The efficiency of polymerase chain reaction can be improved with the use of graphene based nanofluid. Nanofluids have tunable optical properties and due to these properties, they are used in solar collectors. Nanofluids are also used in biomedical, transportation, microfluids and manufacturing. Bioconvection is a phenomenon that occurs when microorganisms (which are denser than water) swim upward on average. Due to up swimming the microorganisms involved such as gyrotactic microorganisms like algae tend to concentrate in the upper portion of the fluid layer thus causing a top heavy density stratification that often becomes unstable. The study of nanofluid bioconvection describing the spontaneous pattern formation and density stratification induced by the simultaneous interaction of the denser self-propelled microorganisms, nanoparticles and buoyancy forces seems necessary. These microorganisms may include

gravitaxis, gyrotaxis or oxytaxis organisms. The addition of gyrotactic microorganisms into the nanofluid increases its stability as a suspension. The bioconvection process is a mesoscale phenomenon in which the motion of gyrotactic motile microorganisms induces a microscopic motion (convection) in the fluid. The hydrodynamic convection induced by the oxytactic microorganisms which are oxygen consumers, leads to a flow system which transport cell and oxygen from the upper fluid region to the lower fluid region. Bioconvection has been studied extensively due to its wide applications in the modeling oil, gas-bearing sedimentary basin, microbial enhanced oil recovery and bio-microsystems. Stratification is a deposition (formation) of layers which occur as result of different fluids mixtures, temperature variation, densities difference or concentration differences which occur in fluids. Physically, heat and mass transfer analysis run concurrently, it is of great interest to explore the mechanism of double stratification (thermal and mass stratifications) on the convective transport in nanofluid. These draw the attention of researchers such as due to its frequent occurrence in various industrial and engineering processes namely heat rejection into the surrounding (environment) via rivers, lakes and seas, also thermal energy storage systems via solar ponds, condenser of power plants, industrial composition, manufacturing processing and heterogeneous composition in food, atmospheric density stratification, etc. Stratification is a phenomenon which has key contribution in plenty of industrial and natural processes. Concentration and temperature variations or fluids having different densities are responsible for the generation of stratification phenomenon. Simultaneously occurring of both mass and heat transfer gives rise to double stratification. Salinity stratification in water reservoirs and rivers, industrial manufacturing and food processes, heterogeneous mixtures in atmosphere are some examples of stratification. It also plays a key role in controlling the concentration and temperature variations of oxygen and hydrogen in ponds and lakes which can affect growth rate in different species. Due to this reason stratification can play an important role in ponds and lakes. The effect of stratification is an important aspect in heat and mass transfer, and it has been studied by several researchers. Stratification of fluids arises due to temperature variation, concentration differences, or presence of different fluids of different densities. In practical situations where heat and mass transfer run simultaneously, it is important to investigate the effect double stratification on the convective transport in nanofluids. Stratified fluids are ubiquitous in nature, present in almost any heterogeneous fluid

body. Examples include thermal stratification of reservoirs and oceans, salinity stratification in estuaries, rivers, groundwater reservoirs, and oceans, heterogeneous mixtures in industrial, food, and manufacturing processing, density stratification of the atmosphere, and uncountable similar examples. In the presence of gravity, these density differences have a dramatic impact on the dynamics and mixing of heterogeneous fluids. For example, thermal stratification in reservoirs can reduce the vertical mixing of oxygen to the point that bottom water becomes anoxic through the action of biological processes. Preventing, predicting, and solving such a reservoir problem, though dependent on other limnological factors, requires an understanding of the dynamics of stratified fluids. The notion of stratification is essential in lakes and ponds. It is important to control the temperature stratification and concentration differences of hydrogen and oxygen in such environments as they may directly affect the growth rate of all cultured species. Also, the analysis of thermal stratification is important for solar engineering because higher energy efficiency can be achieved with better stratification. It has been shown by researchers that thermal stratification in energy storage may considerably increase system performance.

1.2 Literature review

Over the past few years, the requirement to model and shape the fluid that comprises rotating micro constituents has given rise to the micropolar fluid theory. The fluids that couple the particles rotatory motion and macroscopic velocity field are known as Micro-polar fluids. Such fluids are made of stiff particles that are cuddled in a viscous or sticky medium. Examples of such fluid are blood flow, bubbly liquid and ferro fluid. The industrial applications of these fluids like biological structures, lubricant fluids, and polymer solutions have also great importance. A lot of research is done on micropolar fluids theory around the world. This concept was first given by Eringen [1]. Taking into the limitations of thermodynamics, the boundary conditions and main equations of the micro polar fluids have been derived and solved for the channel flow. The flow of blood in an artery can be modeled by such fluids because of micro rotational vector that is engaged in such type of the fluids. Nazar et al. [2] studied the two dimensional stagnation point flow of micropolar fluid induced by stretching sheet. The heat and mass transfer features

of magnetohydrodynamic (MHD) flow of micropolar fluid due to stretching surface saturated in a porous medium was reported by Pal and Chatterjee [3]. Later, Mabood et al. [4] added the effect of chemical reaction in micropolar fluid past a stretching sheet near the stagnation point. They noticed a strong impact of chemical reaction on micropolar fluid concentration. Recently Nadeem et al. [5] carried out heat transfer analysis in three dimensional flow of micropolar fluid generated due to exponential surface. Some other related work on micropolar fluid can be found in $[6-9]$.

On the other hand, the study of nanofluid heat transfer flow has attracted considerable attention. Nanofluid is a liquid that is made by propagation of strong particles with dimensions less than 100 nm in fluids. A nanofluid low thermal conductivity is one of its striking parameters that can restrain the performance of heat transfer. Because of their low heat transfer properties, normal heat transport fluids such as water, ethylene glycol, and engine oil have limited heat transfer capabilities and are therefore unable to meet today's cooling requirements. Suspended nanoparticles can improve the fluid flow and heat transfer characteristics of the base fluids. Necessary studies must be conducted before extensive application for nanofluids can be encountered. Keeping in view of its applications, Yadav et al. [10] investigated electrically conducting flow of nanofluid in the presence of internal heating. The effect of magnetic field on viscoelastic nanofluid flow was explored by Farooq et al. [11]. They have chosen viscoelastic fluid as a base fluid for nanoparticles and observed that the behavior of thermophoresis and Brownian motion parameters on nanoparticles concentration is opposite. Sheikholeslami et al.[12] and Sheikholeslami [13] theoretically analyzed the magneto nanofluid in the absence and presence of porous medium, respectively. Their output reveals that the temperature gradient of nanofluid augments with rise of Hartmann number. Pramuanjaroenkij et al. [14] discussed the mixing thermal conductivity model for a single phase boundary layer flow of nanofluid in the presence of viscous dissipation. In their work they have used Cu–water, CuO–water, and Al2O3–water nanofluids as working fluids in a rectangular channel.

Lu et al. [15] discussed the micropolar nanofluid passed a linear stretched surface under the influence of homogenous and heterogeneous reaction. Nadeem et al. [16] introduced three dimension micropolar nanofluid past an exponential stretching sheet by adding magnetic effect. They solved it numerically by bvp4c function of MATLAB. The impact of thermal and velocity

slip on stagnation point flow of micropolar fluid due to circular cylinder was demonstrated by Abbas et al. [17]. Their findings indicate that more defiance in the fluid was observed with increment in velocity slip parameter due to which the shear stress and heat transfer rate reduced. Sheikholeslami et al. [18] analyzed the heat transfer transport of alumina nanofluid in a duct. The numerical solutions were found using Runge-Kutta method. The influence of magnetic field on micropolar nanofluid in the presence of hall current was studied by Shah et al. [19]. They have considered the flow between two parallel plates rotating in its own axis and observed that thermophoresis impact is the same on temperature and concentration profiles. In the rotating system, the three dimensional flow of micropolar nanofluid between parallel and horizontal plates in the presence of heat generation/absorption was reported by Khan et al. [20]. Sadiq et al. [21] found numerical solutions of MHD flow of micropolar fluid in the presence of nanoparticles via Runge-Kutta method. Some interesting features of nanofluid can also be seen in [22] − [26]

The key function of the thermal radiation is to control the transfer of heat procedures. By monitoring heat aspects to a particular range, one can improve the attributes and quality of the ultimate product. In transfer of heat flow, the influence of thermal radiation was extraordinarily significant for a system operating at above average temperature and where radiation from heated walls and working fluid is confronted. An important alteration of the temperature at the walls and away from the walls overstress this entire procedure and show up the value of thermal radiations. The ultimate product's preferred value and quality extremely depends upon understanding with suitable part of the radiative flow over that specific system. Hayat et al. [27] discussed the effects of thermal radiation mixed convection flow near stagnation point under the influence of magnetic field. They found the series solution using homotopy analysis method (HAM) and analyzed the problem for both assisting and opposing flow. The impact of chemical reaction on radiative flow of viscous fluid over a permeable surface inside a porous medium was investigated by Pal and Talukdar [28]. Bhattacharyya and Layek [29] illustrated the effect of thermal radiation on heat transfer flow past a shrinking sheet. The influence of magnetic field on radiative flow of Jeffery nanofluid due to exponentially stretching surface was deliberated by Hussain et al. [30]. Ramzan and Bilal [31] demonstrated the effect of thermal radiation on electrically conducting unsteady flow of second grade nanofluid induced by stretching surface.

Hayat et al. [32] investigated three dimensional flow of viscoelastic nanofluid in the presence of non-linear thermal radiation. The influence of thermal radiation on boundary layer flow of Jeffer nanofluid in the presence of heat generation and absorption was presented by Ramzan et al. [33]. In another study, Pal and Mandal [34] analyzed the influence of thermal radiation on magnetic flow of micropolar nanofluid due to stretching surface with heat source and sink. They noticed an opposite behavior on velocity and temperature profiles by mixing nanoparticles to the working fluid. Siddiq et al. [35] and Ghadikolaei et al. [36] discussed the linear and nonlinear thermal radiation phenomenon in electrically conducting flow of micropolar nanofluid, respectively.

From the above literature survey, it is evident that less attention is paid towards the effect of nonlinear thermal radiation on micropolar nanofluid. However, no work is done so far on bioconvective MHD flow of micropolar nanofluid in the presence of nonlinear thermal radiation and joule heating. The aim of present analysis is to fill this gap and analyze the influence of thermal radiation on bioconvective MHD flow of micropolar nanofluid with joule heating effects. The velocity slip at boundary wall is also taken into consideration. The series solutions of transformed governing equations are obtained via homotopy analysis method. The results are displayed graphically and discussed.

Chapter 2

Basic preliminaries and laws

This chapter contains some elementary definitions, concepts and laws that are helpful in understanding the works in the second and third chapters.

2.1 Fluid

A material which deforms continuously when shear force is utilized. Gases and liquids are examples of fluid.

2.1.1 Liquid

A type of fluid which has a certain volume however no certain shape *e.g.* blood, water and milk etc.

2.1.2 Gas

A fluid which has no certain shape and volume is known as gas. Nitrogen, hydrogen and oxygen are examples of gases.

2.2 Fluid mechanics

The physical science's branch that deals with the behavior of fluid in motion or in rest. It can be further subdivided in to two branches as follows:

2.2.1 Fluid statics

It describe the properties of fluid that are at rest.

2.2.2 Fluid dynamics

Fluid dynamics studies the features of fluid that are in the state of motion.

2.3 Stress

It is defined as the surface force that act on the unit area within the body which is deformable. It's unit in SI system is Nm^{-2} or $kg/m.s^2$ and its dimension is $\left[\frac{M}{LT^2}\right]$. Stress can be further divided into two types:

2.3.1 Shear stress

Stress is recognized as shear stress when the force acts parallel to the unit area of the surface.

2.3.2 Normal stress

Stress is known as normal stress when the force acts normal to the surface of unit area.

2.4 Strain

A quantity that is used to measure the distortion or deformation of an object when a force acts on it.

2.5 Flow

Flow is described as a material that deform continuously or smoothly under the effects of various type of forces. There are two ways to explain the flow:

2.5.1 Laminar flow

When fluid is flowing in the manner that various layers of fluid never cross each other and the velocity at each point is constant is called as laminar flow.

2.5.2 Turbulent flow

When fluid is flowing in the manner that various layers of fluid cross each other and velocity at each point deviates with the magnitude and direction is called Turbulent flow.

2.6 Viscosity

An intrinsic property of the fluid which measures the resistance of fluid against any gradual distortion or deformation when different forces acts on it is known as viscosity. There are two ways to express the viscosity.

2.6.1 Dynamic viscosity

The property of fluid which measures the fluid's resistance against any distortion or deformation when a force acts on it. Mathematically, it can be stated as:

$$\text{viscosity } (\mu) = \frac{\text{shear stress}}{\text{gradient of velocity}}. \tag{2.1}$$

Its SI unit is Ns/m^2 and dimension is $\left[\frac{M}{LT}\right]$.

2.6.2 Kinematic viscosity

Kinematic viscosity expresses the ratio of dynamic viscosity (μ) to the density of fluid (ρ). Mathematically, it is denoted by:

$$\nu = \frac{\mu}{\rho}. \tag{2.2}$$

Its SI unit is m^2/s and its dimension is $\left[\frac{L^2}{T}\right]$.

2.7 Newton's law of viscosity

It describes the shear force that deforms the fluid element directly and linearly proportional to the gradient of the velocity. Mathematically, it can be stated as:

$$\tau_{yx} \propto \frac{du}{dy}, \tag{2.3}$$

or

$$\tau_{yx} = \mu \left(\frac{du}{dy} \right), \tag{2.4}$$

in which τ_{yx} denotes the shear force applied on the element of fluid and μ represents the proportionality constant and $\frac{du}{dy}$ is shear rate.

2.7.1 Newtonian fluids

Newtonian fluids are those that satisfy the Newton's law of viscosity and the value of μ is constant. In such fluids shear force τ_{yx} is linearly proportional to the gradient of velocity $\left(\frac{du}{dy}\right)$. Glycerine, water, air and kerosene are some common examples of such fluids.

2.7.2 Non-Newtonian fluids

Such fluids for which Newton's law of viscosity don't hold are the non-Newtonian fluids. Here, direct and nonlinear relationship exists among the shear stress τ_{yx} and gradient of the velocity. Mathematically, it is specified as:

$$\boldsymbol{\tau}_{yx} \propto \left(\frac{du}{dy} \right)^{n}, \; n \neq 1, \tag{2.5}$$

or

$$\boldsymbol{\tau}_{yx} = \eta_1 \frac{du}{dy}, \text{ and } \eta_1 = k_2 \left(\frac{du}{dy} \right)^{n-1}, \tag{2.6}$$

where η_1, n and k_2 denote apparent viscosity, index of flow behavior and consistency index respectively. For $n = 1$ Eq. (1.6) converts to Newton's law of viscosity. Ketchup, paints and honey describe the non-Newtonian fluid behavior. Such fluids are characterized mainly into three types i.e. (i) differential type (ii) integral type (iii), and rate type.

2.8 Rate type fluids

Fluids that depict the impacts of retardation and relaxation times are known as rate type fluids. Some common examples of rate type fluid models are Burgers, Oldroyd and Maxwell and Jeffery fluids etc.

2.8.1 Retardation Time

When the shear stress is applied, an opposing force is produced and a time is required to balance this force is known as retardation time.

2.8.2 Relaxation Time

When the stress is applied, then a system from an equilibrium position goes to perturb position. Once the stress is taken off, time required for a perturb system back to an equilibrium position is known as relaxation time.

2.9 Joule heating

Joule heating (also stated to as ohmic or resistive heating) defines the process where the energy of an electric current is transformed into heat as it flows through a resistance.

2.10 Magnetohydrodynamics (MHD)

The word magnetohydrodynamics is combination of the words magneto means magnetic, hydro means water or liquid and dynamic refer to the motion of an object by force. Magnetohydrodynamics is the branch in which we study the dynamics of the high conducting fluids where the magnetic field is present. Blood, liquid metals and salt water are some examples of MHD fluids. Its parameter is called as Hartmann.

2.11 Micropolar fluids

Micropolar fluids are fluids with microstructures. They belong to a class of fluids with a nonsymmetric stress tensor. Micropolar fluids consist of rigid, randomly oriented or spherical particles with their own spins and microrotations, suspended in a viscous medium. Physical examples of micropolar fluids can be seen in ferrofluids, blood flows, bubbly liquids, liquid crystals, and so on, all of them containing intrinsic polarities.

2.12 Nanofluid

A nanofluid is a fluid comprising nanometer-sized particles, known as nanoparticles. Such fluids are persuaded colloidal suspensions of nanoparticles in the base fluid. The nanoparticles consumed in nanofluids were naturally made of carbides, oxides, metals, or carbon nanotubes. Some common base fluids are water, oil and ethylene glycol.

2.13 Stratification

Sometimes the mechanism of deformable density happened/appeared in the shallow fluid medium owing to change in the state of concentration, pressure, temperature and dissolved substances termed as stratification. It is witnessed that in case of stratification, density is the function of space variable as well as time. By cause of which layer formation occurs.

2.14 Thermal stratification

It happens as result of temperature imbalance, which provide rise to density imbalance in the fluid medium. Commomly, the reasons are thermal energy from heated bodies e.g, sun.

2.15 Concentration stratification

This type of stratification has application in many mechanism like transportation in the sea where stratification occurs due to salinity imbalance. As a result of existence of various fluids, a stable standpoint arises when the lighter fluids stands over the denser one.

2.16 Microelectromechanical system

A MEMS (micro-electro-mechanical-system) is a mini machine which has both electronic and mechanical components. The physical dimensions of a MEMS can vary from several milli-meters to less than 1 micro-meter.

2.17 Magnetic field

A magnetic field is a vector field which defines the magnetic impact of magnetized materials and electrical currents.

2.18 Electric field

An electric field (occasionally abbreviated as E-field) is a vector field neighboring an electric charge which exerts force on further charges, repelling or attracting them. Mathematically, the electric field is a vector field which associates to every point in space the force, known as the Coulomb force, which would be experienced per unit of the charge by an infinitesimal test charge at that point. In the SI system the units of the electric field are Newtons per coulomb (N/C), or volts per meter (V/m).

2.19 Uniform magnetic field

When magnetic field lines are parallel then magnetic force experienced by an object is same at all points in that field and such a field is called uniform magnetic field. For example a bar magnet's strength is greater at its poles[non uniform] however inside a solenoid the magnetic field lines are parallel.

2.20 Incompressible flow

In fluid mechanics or more commonly continuum mechanics, incompressible flow (isochoric flow) states a flow in which the material density is constant within a fluid cartonl or an infinitesimal volume which moves with the flow velocity. In other words incompressible flow means a small elements of fluid are not compressible *i.e.* their volume is constant.

2.21 Angular velocity

Angular velocity is the rate of velocity at which an object or a particle is rotating around a center or a specific point in a given time period. It is also known as rotational velocity. Angular

velocity is measured in angle per unit time or radians per second (rad/s). The rate of change of angular velocity is angular acceleration. It is typically represented by the symbol omega (ω, sometimes Ω).

2.22 Electrical conductivity

Electrical conductivity is the measure of the amount of an electrical current a material can carry or its capacity to carry a current. Electrical conductivity is also called as specific conductance. Conductivity is an intrinsic property of any material. Electrical conductivity is symbolized as σ and has SI units of siemens per meter (S/m).

2.23 Specific heat

The specific heat is the amount of heat per unit mass essential to increase the temperature by one degree Celsius. The relationship among temperature and heat change is typically expressed in the form shown below where Q_1 is heat added, c is the specific heat, m is mass and ΔT is change in temperature.

$$Q_1 = cm\Delta T \tag{2.7}$$

2.24 Stefan-Boltzmann constant

The Stefan-Boltzmann constant (also Stefan's constant), a physical constant represented by the Greek letter σ (sigma), is the proportionality constant in the Stefan-Boltzmann law: the total intensity radiated over all wavelengths increases as the temperature increases, of a black body that is proportional to the fourth power of the thermodynamic temperature.

2.25 Heat transfer coefficient

The heat transfer co-efficient or film co-efficient, or film effectiveness, in thermodynamics and in mechanics is the constant of proportionality between the thermodynamic driving force and the heat flux for the heat flow (*i.e.* the temperature difference, ΔT): The total heat transfer rate

for combined modes is typically expressed in terms of an overall heat transfer or conductance coefficient. In that case, the heat transfer rate is:

$$\dot{Q} = hA\left(T_2 - T_1\right), \tag{2.8}$$

where

A: surface area where the heat transfer takes place,

T_2: temperature of the surrounding fluid,

T_1: temperature of the solid surface.

The general definition of the heat transfer coefficient is:

$$q = d\dot{Q}/dA, \tag{2.9}$$

where q: heat flux, W/m^2; *i.e.*, thermal power per unit area,

h: heat transfer coefficient, $W/\left(m^2.K\right)$

ΔT: difference in temperature between the solid surface and surrounding fluid area, K

It is used in calculating the heat transfer, characteristically by phase transition or convection among a fluid and a solid. The heat transfer coefficient has the SI units in watts per squared meter kelvin: $W/(m^2K)$.

2.26 Ambient temperature

Ambient temperature is the air temperature of an object or environment. In computing, ambient temperature denotes to the air temperature nearby computing equipment.

2.27 Material parameter

Material Parameters are distinct kind of material expression nodes which allow you to alter the look of a material deprived of having to recompile the material to see the results. Material parameter expression nodes work like any other material node that you might use in the material graph but with one key difference.

2.28 Heat flux

Heat flux or thermal flux, occasionally referred to as heat flux density or heat flow rate intensity is a flow of energy per unit area per unit time. In the SI, its units are watts per square metre$\left(W.m^{-2}\right)$. It has both a magnitude and direction, and thus it is a vector quantity. To express the heat flux at a certain point in space, one can takes the limiting case where the size of the surface turn into infinitesimally small. Heat flux is generally denoted $\overrightarrow{\phi}$, the subscript q specifying heat flux, as opposed to momentum flux or mass.

2.29 Arbitrary constant

An arbitrary constant is that whose value can be expected to be anything, just so long as it does not depend on the additional variables in an expression or equation. A constant which is not arbitrary can typically just take one value (or may be, a set of possible values).

2.30 Density

Density is expressed as mass of a material per unit volume. This extent is used to measure that how much stuff of the material present in a unit volume. Mathematically,

$$\rho = \frac{\mu}{\nu}. \tag{2.10}$$

The SI unit of density is kg/m^3, where ρ is density, μ is dynamic viscosity and ν is kinematic viscosity.

2.31 Pressure

Pressure is defined as a magnitude of force applied perpendicular to a surface per unit area. Mathematically expression for the pressure is given by:

$$P = \frac{F}{A}. \tag{2.11}$$

The SI unit of pressure is N/m^2.

2.32 Thermal conductivity

Thermal diffusivity is a material's specific property for signalizing the heat conduction. This value defines that how much heat is transferred in a material. From the Fourier's law for heat conduction it can be expressed as a ratio of heat transferred with unit thickness of a substance per unit time and per unit surface area divided by the temperature difference. Mathematically,

$$k_7 = \frac{Q_L}{A(\Delta T)} \ . \tag{2.12}$$

The SI unit is $kgm/s^3.k$ and its dimension is $(\frac{ML}{T^3\theta})$, where Q_L is heat transferred with unit thickness of a substance per unit time, k_7 is thermal conductivity and ΔT is the temperature gradient.

2.33 Convective boundary condition

Convective boundary condition is sometime called Robin boundary conditions. This kind of conditions were usually expressed on a wall. Mathematically, these are stated as

$$k\left(\frac{\partial T}{\partial m_i}\right)_{x_i} = h\left(T_f(x_i,t) - T_w(x_i,t)\right). \tag{2.13}$$

This equation utters that condition is equal to convection, where h specifies the heat transfer coefficient , x_i is the coordinate at the boundary , T_f convective fluid temperature and T_w the wall temperature.

2.34 Dimensionless numbers

2.34.1 Radiation parameter

The radiation parameter describes the relative influence of conduction heat transfer to thermal radiation transfer and that can be stated as follows:

$$R = \frac{4\sigma_1^* T_\infty^3}{k_1 k^*}, \tag{2.14}$$

in which k^* stands for mean absorption coefficient, k_1 is thermal conductivity, T_∞ describes ambient temperature and σ_1^* signifies the reaction rate constant.

2.34.2 Prandtl number

The ratio of Momentum diffusivity (ν) to thermal diffusivity (α) is called as Prandtl number. Mathematically, it can be stated by:

$$\mathrm{Pr} = \frac{\nu}{\alpha} = \frac{\mu c_p}{k_3}, \tag{2.15}$$

where μ signifies the dynamic viscosity, c_p represents the specific heat and k_3 stands for thermal conductivity. In heat transfer, Prandtl number is used to control the thicknesses of momentum and thermal boundary layers.

2.34.3 Hartmann number

It expresses the connection among frictional force and viscosity induced by magnetism. It plays a vital role in the magneto-hydrodynamics. Hartmann number is the ratio of electromagnetic to the viscous force *i.e.*

$$M_1^2 = M = \frac{\sigma B_0^2}{\rho a}, \tag{2.16}$$

where B_0 is the applied magnetic field strength, σ the electrical conductivity and ρ stands for density.

2.34.4 Skin friction coefficient

When fluid is passing across a surface, particular amount of drag emerges that is known as Skin friction. It occurs among the solid's surface and fluid that leads to decelerate the motion of fluid. The Skin friction co-efficient can be expressed as:

$$C_{f_x} = \frac{\tau_w}{\frac{1}{2}\rho U_w^2}, \tag{2.17}$$

in which τ_w stands for wall shear stress, ρ stands for density and U_w represents the velocity.

2.34.5 Nusselt number

The dimensionless number which signifies the relation between convection and conduction heat transfer coefficients through the boundary/wall is characterized as Nusselt number. Mathematically,

$$Nu_x = \frac{xq_w}{k_4(T_f - T_0)}, \tag{2.18}$$

where q_w stands for heat flux at wall, k_4 for thermal conductivity and T_0 for fluid reference temperature.

2.34.6 Local Sherwood number

It is a mass transfer rate at the wall. Mathematically, ratio of mass transfer by convection to diffusion can be expressed as follows

$$Sh_x = \frac{xq_m}{D_B\,(C_f - C_0)}, \tag{2.19}$$

here D_B Brownian diffusion coefficient, C_f convective fluid concentration and C_0 reference concentration of nano particles.

2.34.7 Peclet number

The Péclet number (Pe) is a class of dimensionless numbers relevant in the study of transport phenomena in a continuum. It is named after the French physicist Jean Claude Eugène Péclet. It is defined to be the ratio of the rate of advection of a physical quantity by the flow to the rate of diffusion of the same quantity driven by an appropriate gradient. In the context of species or mass transfer, the Péclet number is the product of the Reynolds number and the Schmidt number. In the context of the thermal fluids, the thermal Peclet number is equivalent to the product of the Reynolds number and the Prandtl number. The Péclet number is defined as:

$$Pe = \frac{advective\ transport\ rate}{diffusion\ transport\ rate}.$$

For mass transfer, it is defined as:

$$Pe = \frac{bW_c}{D_m}, \tag{2.20}$$

where b is the chemotaxis constant, W_c the maximum cell swimming speed and D_m the microorganisms diffusion coeficient.

2.34.8 Thermophoresis parameter

Thermophoresis is a method that is used to inhibit the mixing of various particles because of a pressure gradient when they move jointly or isolate the mixture of particles after they get mixed up. In a cold surface thermophoresis is positive and it is negative for a hot surface. Mathematically, it can be expressed as

$$N_t = \frac{(\rho c)_p D_T (T_f - T_0)}{(\rho c)_f \ \nu T_\infty}, \tag{2.21}$$

where T_f, T_0 and T_∞ are the convective fluid temperature, fluid reference temperature and ambient temperature , D_T is thermophoretic diffusion coefficient and v the kinematic viscosity.

2.34.9 Brownian motion parameter

Brownian motion happens due to size of the nano-particles in a nano-fluid. It is a nano-scale mechanism which shows the thermal impacts of nano-fluid. Mathematically,

$$N_b = \frac{\tau D_B (C_f - C_\infty)}{\nu}, \tag{2.22}$$

where

$$\tau = \frac{(\rho c)_p}{(\rho c)_f}. \tag{2.23}$$

In the above equation τ is the ratio of effective heat and heat capacity of the nano-particles and fluid respectively, ν the kinematic viscosity. C_f the convective fluid concentration, C_∞ the ambient concentration and D_B the Brownian diffusion coefficient.

2.35 Fundamental laws

The funddamental laws that are used for the flow specification in the subsequential analysis are given below.

2.35.1 Law of mass conservation

It states that the total mass in any closed system will remain constant. Mathematically,

$$\frac{D\rho}{Dt} + \rho\boldsymbol{\nabla}.\mathbf{V} = 0, \tag{2.24}$$

or

$$\frac{\partial\rho}{\partial t} + (\mathbf{V}.\boldsymbol{\nabla})\,\rho + \rho\boldsymbol{\nabla}.\mathbf{V} = 0, \tag{2.25}$$

or

$$\frac{\partial\rho}{\partial t} + \boldsymbol{\nabla}.\,(\rho\mathbf{V}) = 0. \tag{2.26}$$

It is known as the equation of continuity. For the steady flow Eq. (2.25) becomes

$$\boldsymbol{\nabla}.\,(\rho\mathbf{V}) = 0, \tag{2.27}$$

and if the fluid is incompressible then Eq. (2.26) implies that

$$\boldsymbol{\nabla}.\mathbf{V} = 0. \tag{2.28}$$

2.35.2 Law of momentum conservation

It is stated that the total linear momentum of a closed system is constant. Generally, it is given by:

$$\rho\frac{D\mathbf{V}}{Dt} = \text{div}\,\boldsymbol{\tau}^{*}+\rho\mathbf{b}_1, \tag{2.29}$$

where $\boldsymbol{\tau}^{*}$ denotes the Cauchy stress tensor and $\mathbf{b}_1$ stands for body force.

2.35.3 Law of energy conservation

Law of conservation of energy is also known as energy equation and is given by:

$$\rho\frac{D\mathbf{e}}{Dt} = \boldsymbol{\tau}^*.\mathbf{L} - \boldsymbol{\nabla}.\mathbf{q}+\rho r, \tag{2.30}$$

in which $\mathbf{e}$ stands for specific internal energy, $\mathbf{q}$ for heat flux vector and r for thermal radiation. Energy equation without thermal radiation takes the form

$$\rho c_p\frac{DT}{Dt} = \boldsymbol{\tau}^*.\mathbf{L}+k_5\boldsymbol{\nabla}^2T, \tag{2.31}$$

where $\mathbf{e}$ =c_pT, $\mathbf{q} = -k_5\boldsymbol{\nabla}T$, k_5 denotes the thermal conductivity and T for temperature.

2.35.4 Law of concentration conservation

For nanoparticles, the volume fraction equation is stated as:

$$\frac{\partial C}{\partial t} + \mathbf{V}.\boldsymbol{\nabla}\mathbf{C} = -\frac{1}{\rho_p}\boldsymbol{\nabla}.\mathbf{j}_p, \tag{2.32}$$

or

$$\frac{\partial C}{\partial t} + \mathbf{V}.\boldsymbol{\nabla}\mathbf{C} = \mathbf{D}_B\boldsymbol{\nabla}^2\mathbf{C} + \mathbf{D}_T\frac{\boldsymbol{\nabla}^2T}{T_\infty} \tag{2.33}$$

2.36 Homotopy

Homotopy is the fundamental concept of topology. It is a continous mapping in which one function can be continuously converted into the other function. If one function f_1 and other function f_2 are maps from one topological space X into the other Y then there exist F such that

$$F : X \times [0, 1] \to Y, \tag{2.34}$$

where $x \in X$ and

$$F(x,0) = f_1(x),$$

$$F(x,1) = f_2(x), \tag{2.35}$$

F is known as homotopy.

Chapter 3

Radiative and Joule heating effects in the MHD flow of a micropolar fluid with partial slip and convective boundary condition

3.1 Mathematical Formulation

Let's consider a steady 2-dimensional incompressible MHD flow of a micropolar fluid upon a penetrable elongating sheet with a slip velocity. At this point uniform electric and magnetic fields were also exploited to observe the flow performance with convective transfer of heat. Joule heating effects and thermal radiation due to electric and magnetic fields were also entertained. The boundary layer equations representing the system are:

$$\frac{\partial u}{\partial x} + \frac{\partial v}{\partial y} = 0, \tag{3.1}$$

$$u\frac{\partial u}{\partial x} + v\frac{\partial u}{\partial y} = (\frac{\mu + k}{\rho})\frac{\partial^2 u}{\partial y^2} + \frac{k}{\rho}\frac{\partial N}{\partial y} + \frac{\sigma}{\rho}(E_0 B_0 - B_0^2 u), \tag{3.2}$$

$$u\frac{\partial N}{\partial x} + v\frac{\partial N}{\partial y} = \frac{\gamma^*}{\rho j}\frac{\partial^2 N}{\partial y^2} - \frac{k}{\rho j}\left(2N + \frac{\partial u}{\partial y}\right), \tag{3.3}$$

$$u\frac{\partial T}{\partial x}+v\frac{\partial T}{\partial y}=\frac{k_1}{\rho c_p}\frac{\partial^2 T}{\partial y^2}+\frac{(uB_0-E_0)^2\sigma}{\rho c_p}+\frac{16\sigma^*}{3k^*}T_\infty^3\frac{\partial^2 T}{\partial y^2}, \tag{3.4}$$

with the following boundary conditions

$$u=ax+\alpha^*[(\mu+k)\frac{\partial u}{\partial y}+kN],\quad v=v_w,\quad N=-n\frac{\partial u}{\partial y},\ -k\frac{\partial T}{\partial y}=h_f\left(T_f-T\right),\quad \text{at}\quad y=0,$$

$$u\to 0,\quad N\to 0,\quad T\to T_\infty,\quad \text{as}\quad y\to\infty. \tag{3.5}$$

Where, n is a constant and $0\le n\le 1$. It is noted that $n=0$ represents strong concentration, $n=1/2$ indicates that anti-symmetrical part of the stress tensor vanishes which tends to weak concentration. The case $n=1$ is for turbulent flows. On setting

$$\eta=\sqrt{\frac{a}{\nu}}y,\quad \psi=\sqrt{a\nu}xf(\eta),\quad N=ax\sqrt{\frac{a}{\nu}}h(\eta),\quad \theta(\eta)=\frac{T-T_\infty}{T_f-T_\infty}, \tag{3.6}$$

Eq. (3.1) is satisfied automatically, and Eqs. (3.2) to (3.4) take the form

$$(1+K)f'''+ff''-f'^2+Kh'-M^2f'+M^2E=0, \tag{3.7}$$

$$(1+\frac{K}{2})h''+fh'-f'h-K(2h+f'')=0, \tag{3.8}$$

$$(1+\frac{4R}{3})\theta''+Prf\theta'+M^2Ec[f'^2+E^2-2Ef']=0, \tag{3.9}$$

$$f=f_w,\ f'=1+\alpha(1+K)f'',\ h(0)=-nf''(0),\ \theta'(0)=-\gamma\left(1-\theta(0)\right)$$

$$f'(\infty)=0,\ h(\infty)=0,\ \theta(\infty)=0. \tag{3.10}$$

with

$$K=\frac{k}{\mu},\ M_1^2=M=\frac{\sigma B_o^2}{\rho a},\ f_w=-(a\nu)^{-\frac{1}{2}}v_w,\ \alpha=\alpha^*\mu\sqrt{\frac{a}{\nu}},$$

$$Pr=\frac{\nu}{\alpha}=\frac{\mu c_p}{k_3},\quad E^2=\frac{E_0^2}{u_w^2B_0^2},\quad R=\frac{4\sigma^*T_\infty^3}{k^*k_1}. \tag{3.11}$$

The local Skin friction and Nusselt number are defined as:

$$C_{f_x} = \frac{2\tau_w}{\rho(ax)^2}, \quad Nu_x = \frac{xq_w}{k_4(T_f - T_\infty)}, \tag{3.12}$$

where τ_w (wall shear stress) and q_w (heat flux at wall) are given by:

$$\tau_w = \left((\mu + k)\frac{\partial u}{\partial y} + kN\right)_{y=0}, \quad q_w = -k_6\left(\frac{\partial T}{\partial y}\right)_{y=0}.$$

Dimensionless form of the above equations are

$$\frac{1}{2}C_{f_x}\,\mathrm{Re}_x^{1/2} = (1 + (1-n)\,K)\,f''(0), \quad Nu_x/Re_x^{1/2} = -\theta'(0)\,. \tag{3.13}$$

where the local Reynolds number is given by $Re_x = ux/\nu$.

3.2 Series solutions

The choice of HAM requires to define initial guesses and linear operators [37] for questioned series solutions:

$$f_0(\eta) = f_w + \frac{1}{1+\alpha\,(1+K)}\left(1 - e^{-\eta}\right), \; g_0(\eta) = \frac{n}{1+\alpha\,(1+K)}e^{-\eta}, \; \theta_0(\eta) = \frac{\gamma\exp(-\eta)}{1+\gamma}, \tag{3.14}$$

$$\mathcal{L}_f = f''' - f', \; \mathcal{L}_h = h'' - h', \quad \mathcal{L}_\theta = \theta'' - \theta. \tag{3.15}$$

These auxiliary linear operators [38] possesses the ensuing features

$$\mathcal{L}_f(H_1 + H_2e^{-\eta} + H_3e^{\eta}) = 0, \; \mathcal{L}_h(H_4e^{-\eta} + H_5e^{\eta}) = 0, \; \mathcal{L}_\theta(H_6e^{-\eta} + H_7e^{\eta}) = 0, \tag{3.16}$$

in which H_i $(i = 1 - 7)$ symbolize arbitrary constants.

3.2.1 Zeroth-order deformation problems

The zeroth order deformation problems are given as under:

$$(1-p)\,\mathcal{L}_f\left[\hat{f}(\eta;p)-f_0(\eta)\right]=p\hbar_f\mathcal{N}_f\left[\hat{f}(\eta;p),\hat{h}(\eta;p)\right], \tag{3.17}$$

$$(1-p)\,\mathcal{L}_h\left[\hat{h}(\eta;p)-h_0(\eta)\right]=p\hbar_h\mathcal{N}_h\left[\hat{f}(\eta;p),\hat{h}(\eta;p)\right], \tag{3.18}$$

$$(1-p)\,\mathcal{L}_\theta\left[\hat{\theta}(\eta;p)-\theta_0(\eta)\right]=p\hbar_\theta\mathcal{N}_\theta\left[\hat{f}(\eta;p),\hat{h}(\eta;p),\hat{\theta}(\eta,p)\right], \tag{3.19}$$

$$\hat{f}(0;p)=f_w,\qquad \hat{f}'(0;p)=1+\alpha\,(1+K)\,\hat{f}''(0;p),$$

$$\hat{f}'(\infty;p)=0,\quad \hat{h}(0;p)=-n\hat{f}''(0;p),\quad \hat{h}(\infty;p)=0,$$

$$\hat{\theta}'(0,p)=-\gamma\,(1-\theta(0,p)),\qquad \hat{\theta}(\infty,p)=0, \tag{3.20}$$

$$\begin{aligned}\mathcal{N}_f[\hat{f}(\eta,p)] &= (1+K)\,\frac{\partial^3\hat{f}(\eta,p)}{\partial\eta^3}-\left(\frac{\partial\hat{f}(\eta,p)}{\partial\eta}\right)^2+\\ &\quad \hat{f}(\eta,p)\frac{\partial^2\hat{f}(\eta,p)}{\partial\eta^2}+K\frac{\partial\hat{h}}{\partial\eta}(\eta,p)-M^2\frac{\partial\hat{f}(\eta,p)}{\partial\eta}+M^2E,\end{aligned} \tag{3.21}$$

$$\begin{aligned}\mathcal{N}_h[\hat{f}(\eta,p),\hat{h}(\eta,p)] &= \left(1+\frac{K}{2}\right)\frac{\partial^2\hat{h}(\eta,p)}{\partial\eta^2}+\hat{f}(\eta,p)\frac{\partial\hat{h}(\eta,p)}{\partial\eta}-\\ &\quad \frac{\partial\hat{f}(\eta,p)}{\partial\eta}\hat{h}(\eta,p)-2K\;\hat{h}(\eta,p)-K\frac{\partial^2\hat{f}(\eta,p)}{\partial\eta^2},\end{aligned} \tag{3.22}$$

$$\mathcal{N}_\theta[\hat{\theta}(\eta,p),\hat{f}(\eta,p)]=\left(1+\frac{4K}{3}\right)\frac{\partial^2\hat{\theta}(\eta,p)}{\partial\eta^2}+\mathrm{Pr}\,\hat{f}(\eta,p)\frac{\partial\hat{\theta}(\eta,p)}{\partial\eta}$$

$$+MEc\left(\frac{\partial\hat{f}(\eta,p)}{\partial\eta}\right)^2+MEc\left(E^2-2E\frac{\partial\hat{f}(\eta,p)}{\partial\eta}\right). \tag{3.23}$$

where p is an embedding parameter, $\hbar_f$, $\hbar_h$ and $\hbar_\theta$ are the non-zero auxiliary parameters and $\mathcal{N}_f$, $\mathcal{N}_h$ and $\mathcal{N}_\theta$ the nonlinear operators. For $p = 0$ and $p = 1$ we have

$$\hat{f}(\eta; 0) = f_0(\eta), \ \hat{f}(\eta; 1) = f(\eta), \tag{3.24}$$

$$\hat{h}(\eta; 0) = h_0(\eta), \ \hat{h}(\eta; 1) = \hat{h}(\eta), \tag{3.25}$$

$$\hat{\theta}(\eta, 0) = \theta_0(\eta), \ \hat{\theta}(\eta, 1) = \theta(\eta), \tag{3.26}$$

and $\hat{f}(\eta, p)$, $\hat{h}(\eta, p)$ and $\hat{\theta}(\eta, p)$ vary from $f_0(\eta)$, $h_0(\eta)$, $\theta_0(\eta)$ to $f(\eta)$, $h(\eta)$ and $\theta(\eta)$ when p varies from 0 to 1. By Taylor's series expansion, we obtain

$$\hat{f}(\eta, p) = f_0(\eta) + \sum_{m=1}^{\infty} f_m(\eta) p^m, f_m(\eta) = \frac{1}{m!} \left. \frac{\partial^m \hat{f}(\eta; p)}{\partial \eta^m} \right|_{p=0}, \tag{3.27}$$

$$\hat{h}(\eta, p) = h_0(\eta) + \sum_{m=1}^{\infty} h_m(\eta) p^m, \ h_m(\eta) = \frac{1}{m!} \left. \frac{\partial^m \hat{h}(\eta; p)}{\partial \eta^m} \right|_{p=0}, \tag{3.28}$$

$$\hat{\theta}(\eta, p) = \theta_0(\eta) + \sum_{m=1}^{\infty} \theta_m(\eta) p^m, \ \theta_m(\eta) = \frac{1}{m!} \left. \frac{\partial^m \hat{\theta}(\eta; p)}{\partial \eta^m} \right|_{p=0}, \tag{3.29}$$

where the convergence of above series sturdily influenced by h_f, h_h and h_θ. Selecting h_f, h_h and h_θ in an appropriately manner so that Eqs. $(3.27) - (3.29)$ converge at $p = 1$, and consequently we have

$$\hat{f}(\eta) = f_0(\eta) + \sum_{m=1}^{\infty} f_m(\eta), \tag{3.30}$$

$$\hat{h}(\eta) = h_0(\eta) + \sum_{m=1}^{\infty} h_m(\eta), \tag{3.31}$$

$$\hat{\theta}(\eta) = \theta_0(\eta) + \sum_{m=1}^{\infty} \theta_m(\eta). \tag{3.32}$$

3.2.2 mth-order deformation problems

The subjected problems of the mth order are

$$\mathcal{L}_f \left[f_m(\eta) - \chi f_{m-1}(\eta) \right] = \hbar_f R_{f,m}(\eta), \tag{3.33}$$

$$\mathcal{L}_h\left[h_m(\eta)-\chi_m h_{m-1}(\eta)\right]=\hbar_h R_{h,m}(\eta), \tag{3.34}$$

$$\mathcal{L}_\theta\left[\theta_m(\eta)-\chi_m\,\theta_{m-1}(\eta)\right]=\hbar_\theta R_{\theta,m}(\eta), \tag{3.35}$$

$$\begin{aligned} f_m(0) &= f_w, \quad f'_m(0)=\alpha\,(1+K)\,f''_m, \quad f'_m(\infty)=0, \\ h_m(0) &= -nf''_m(\infty), \quad h_m(\infty)=0,\ \theta'_m(0)-\gamma\theta_m(0)=0, \quad \theta_m(\infty)=0, \end{aligned} \tag{3.36}$$

$$\begin{aligned} R^f_m(\eta) &= (1+K)\,f'''_{m-1}+Kh'_{m-1}-M^2f'_{m-1} \\ &+\sum_{k=0}^{m-1}\left(f_{m-1-k}f''_k-f'_{m-1-k}f'_k\right)+M^2E\,(1-\chi_m)\,, \end{aligned} \tag{3.37}$$

$$R^h_m(\eta)=\left(1+\frac{K}{2}\right)h'''_{m-1}-2Kh_{m-1}-Kf''_{m-1}+\sum_{k=0}^{m-1}\left[f_{m-1-k}h'_k-f'_{m-1-k}h'_k\right], \tag{3.38}$$

$$\begin{aligned} R^\theta_m(\eta) &= \left(1+\frac{4K}{3}\right)\theta''_{m-1}+\sum_{k=0}^{m-1}\left[\Pr f_{m-1-k}\theta'_k+MEcf'_{m-1-k}f'_k\right] \\ &-2EMEcf'_{m-1}+MEcE^2\,(1-\chi_m)\,. \end{aligned} \tag{3.39}$$

$$\chi_m=\begin{matrix} 0 & m\le 1, \\ 1 & m>1. \end{matrix} \tag{3.40}$$

3.3 Convergence Analysis

The series solution (3.29−3.31) includes of auxiliary parameters $\hbar_f$, $\hbar_h$ and $\hbar_\theta$. Such parameters are valuable in monitoring and regulating the convergence of the achieved series solutions. The suitable values of such parameters are reasonably vital to shape the convergent explanations via the homotopy analysis method (HAM). To choose the suitable values of $\hbar_f, \hbar_h$ and $\hbar_\theta$, $\hbar$-curves are drawn that are depicted in figure 3.1 and it is examined that tolerable ranges of $\hbar_f, \hbar_h$ and $\hbar_\theta$ are $-1.7 \le \hbar_f \le -0.7$, $-2.2 \le \hbar_h \le -0.4$ and $-2.3 \le \hbar_\theta \le -0.8$. Table 3.1 expresses the convergence of series solutions of energy equations, micro-rotation and momentum and it demonstrates that the 25^{th} order of guesstimates are adequate for the convergent series

explanations that are in good understanding to graphical illustration shown in figure 3.1.

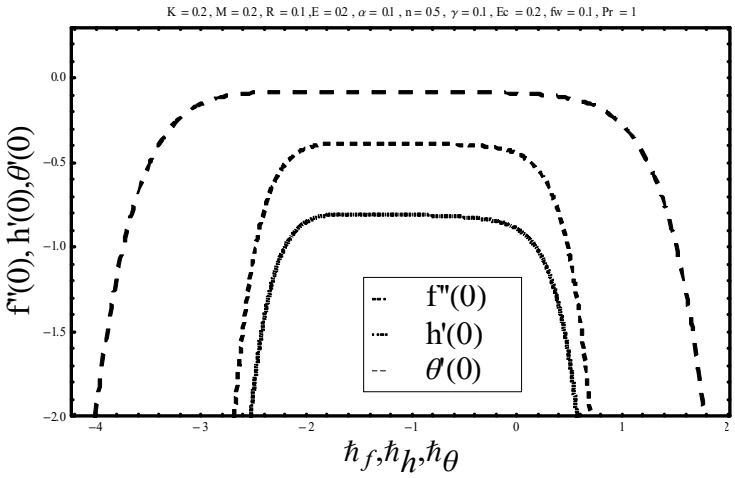

Fig. 3.1: $\hbar-$curves of f, h and θ.

Table 3.1: Convergence of series solution for different order of approximations when $\beta = 0.1$, $K = 0.02$, $M = 0.05$, $\gamma = 0.1, \mathrm{Pr} = 1$, $\hbar_f = \hbar_h = \hbar_\theta = -0.5$.

Order of approximations	$-f''(0)$	$-h'(0)$	$-\theta'(0)$
1	0.85626	0.41857	0.08950
5	0.82136	0.39501	0.08753
10	0.80942	0.38886	0.08678
15	0.80347	0.38632	0.08644
20	0.79963	0.38487	0.08624
25	0.79685	0.38391	0.08612
30	0.79685	0.38391	0.08612

3.4 Discussion

In this particular section we have observed the analysis of various parameters on temperature profiles, micro-rotation and velocity. Impact of Hartmann number M on the velocity profile is shown in figure 3.2. As probable the velocity profile reduces with an increase in Hartmann number. The Lorentz force also increases with an increase in the Hartmann number that opposes

the fluid motion. So, the velocity profile decreases. Performance of slip parameter α on velocity profile is sketched in figure 3.3. Both the velocity and boundary layer thickness decrease with an increase in slip parameter. Figure 3.4 is plotted for the performance of material parameter K on the velocity profile. It is shown that the velocity profile decreases with an increase in the material parameter and boundary layer thickness also decreases. Figure 3.5 is plotted for the effect of electric parameter E on velocity profile. It is clear from the figure that velocity and boundary layer thickness increase with an increase in electric field parameter. Variation of suction parameter f_w on velocity profile is presented in figure 3.6. Velocity profile decreases with an increase in suction parameter. Additional velocity boundary layer thickness is higher for small values of suction parameter. Figure 3.7 is outlined for behavior of Hartmann number M on micro-rotation parameter. The micro-rotation is found to increase when Hartmann number increases. Figure 3.8 is illustrated to observe the effect of slip parameter α on micro-rotation distribution. It is seen that micro-rotation decreases by increasing slip parameter. Effect of material parameter K on micro-rotation is displayed in figure 3.9. It is showed that micro-rotation decreases when material parameter increases. Effect of electric field parameter E on micro-rotation is presented in in figure 3.10. It is witnessed that micro-rotation field reduces when electric field is increased. Analysis of Hartmann number on the distribution of temperature is illustrated in figure 3.11. Temperature distribution and thermal boundary layer thickness are more prominent for higher values of Hartmann number. Effect of electric field E on temperature profile is displayed in figure 3.12. It is obvious that temperature profile increases with an increase in electric field E. Variation of Eckert number Ec on temperature profile is presented in figure 3.13. Here temperature profile increases with an increase in Eckert number Ec. Further thermal boundary layer thickness is higher for large values of Eckert number. Behavior of Pr on temperature profile is examined in figure 3.14. Here the temperature and thermal boundary layer decrease for large Prandtl number. Influence of Biot number γ on temperature profile is inspected in figure 3.15. It is noted that temperature and thermal boundary layer thickness increase due to increase in Biot number. Effect of radiation parameter R on temperature profile is displayed in figure 3.16. It is found that temperature increases due to an increase in radiation parameter. Additionally, the thermal boundary layer thickness is higher for higher values of radiation parameter R. Table 3.2 specifies the behavior of different

parameters on Nusselt number. It is observed that Nusselt number increases with the increase of K, Pr, E, γ and S though it decreases when M, R, α and β are increased.

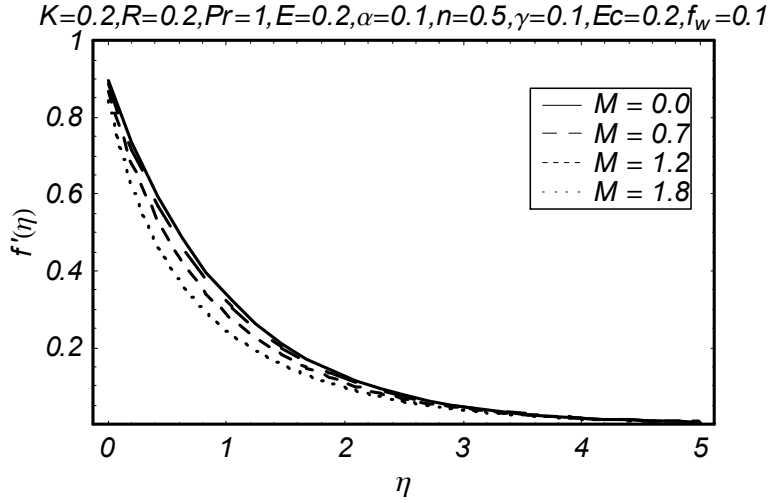

Fig. 3.2: Effect of M on f'.

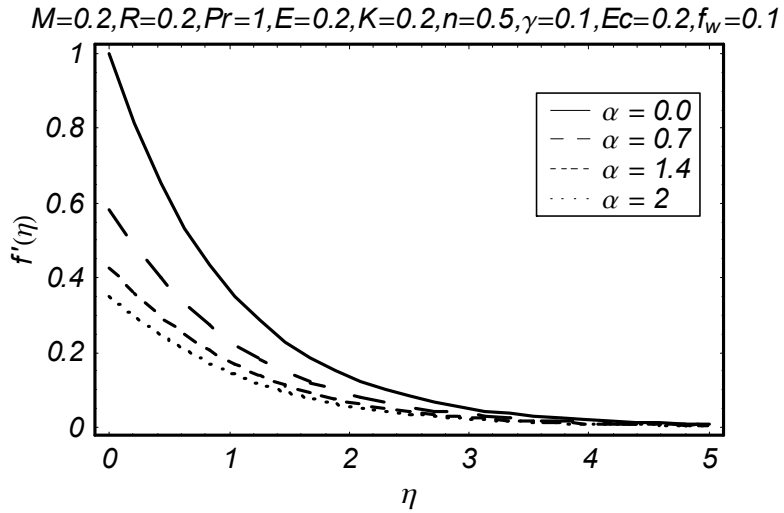

Fig. 3.3: Effect of α on f'.

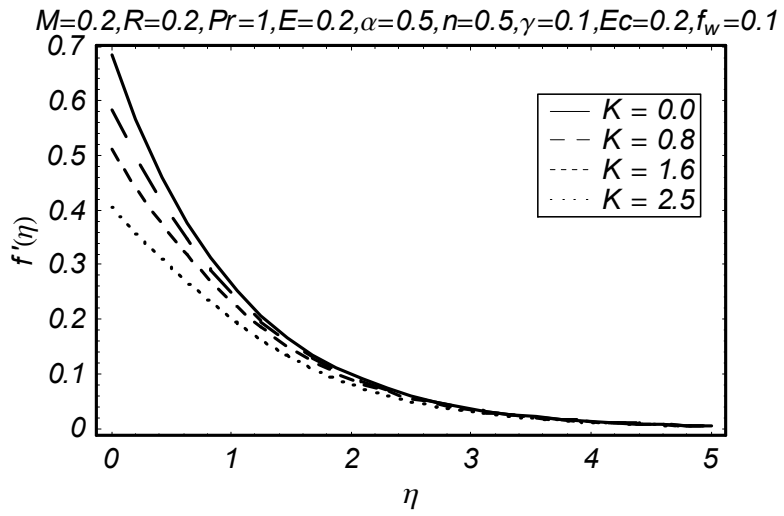

Fig. 3.4: Effect of K on f'.

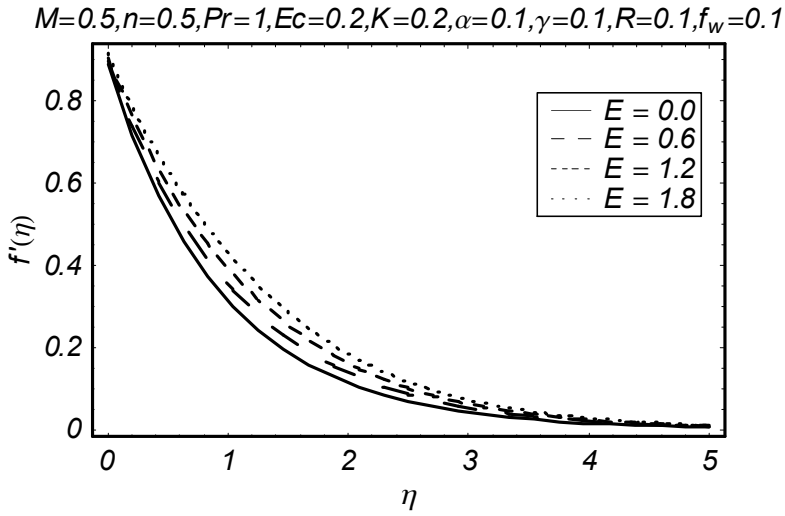

Fig. 3.5: Effect of E on f'.

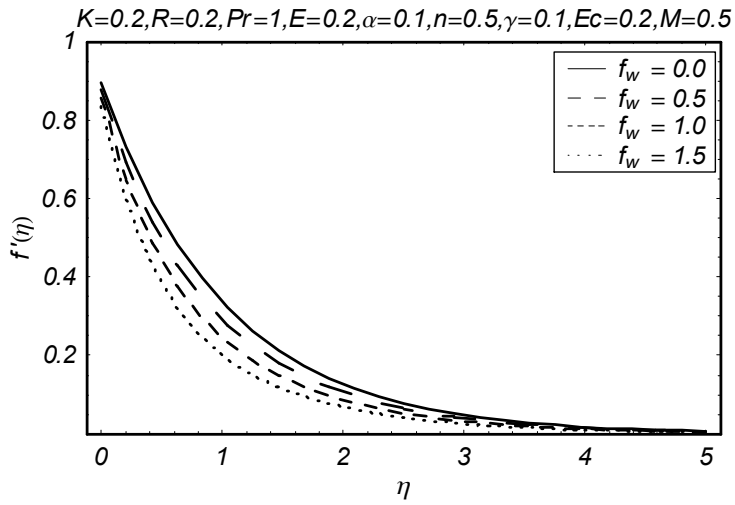

Fig. 3.6: Effect of f_w on f'.

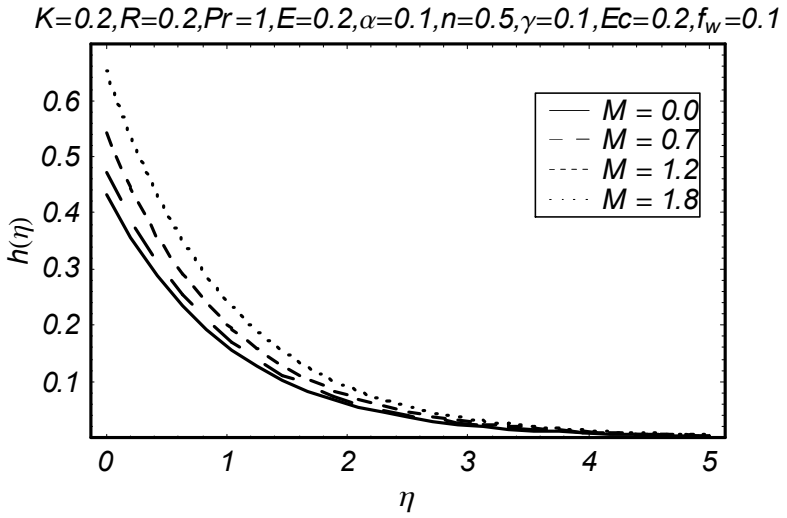

Fig. 3.7: Effect of M on h.

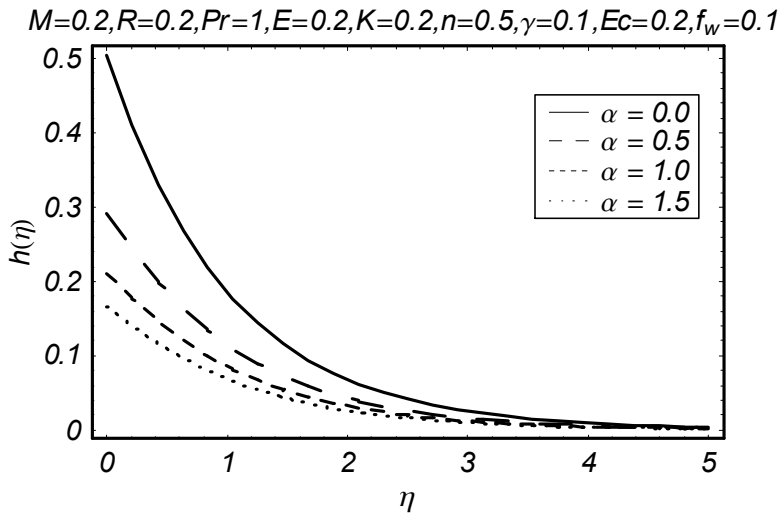

Fig. 3.8: Effect of α on h.

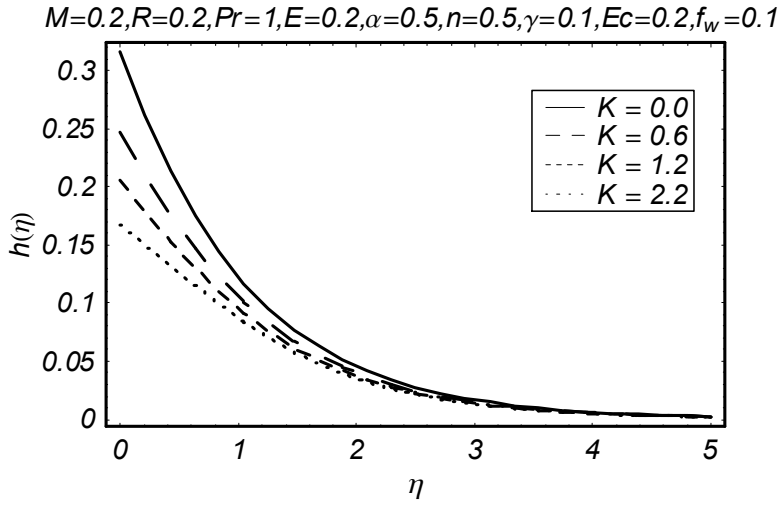

Fig. 3.9: Effect of K on h.

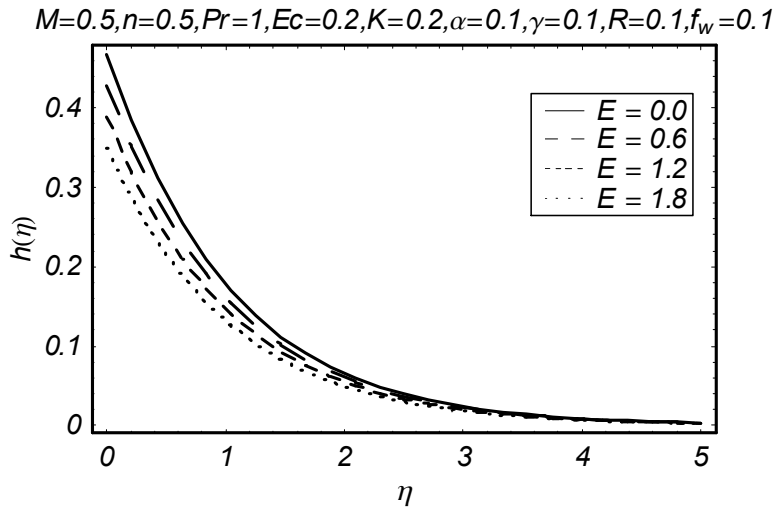

Fig. 3.10: Effect of E on h.

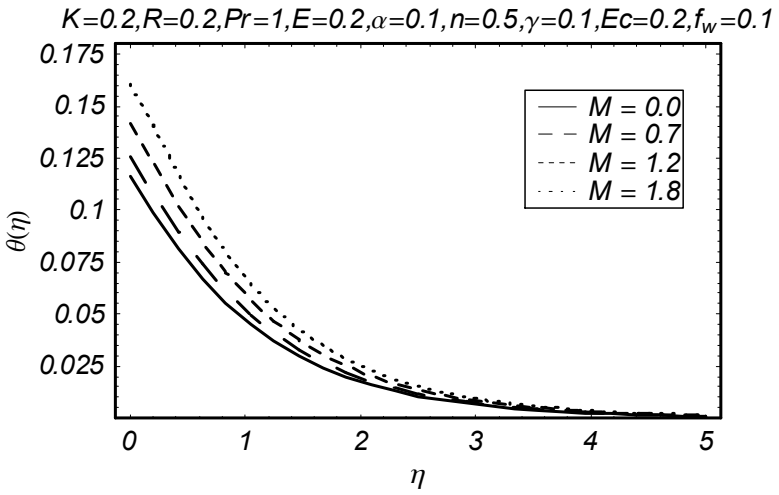

Fig. 3.11: Effect of M on θ.

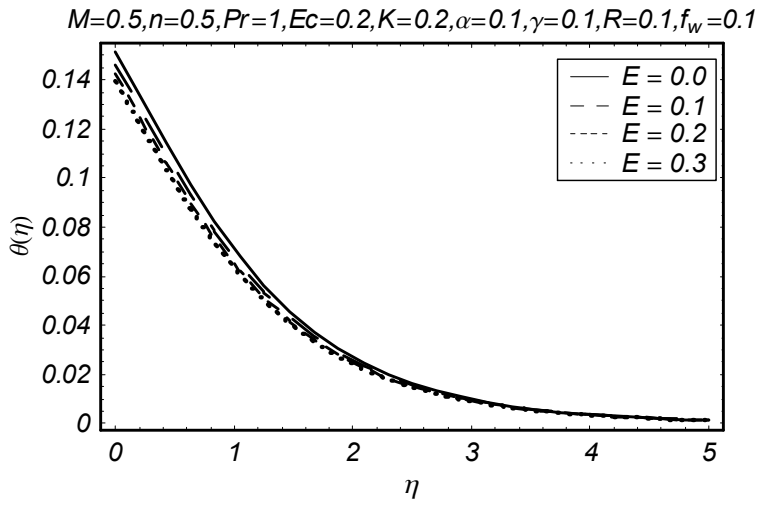

Fig. 3.12: Effect of E on θ.

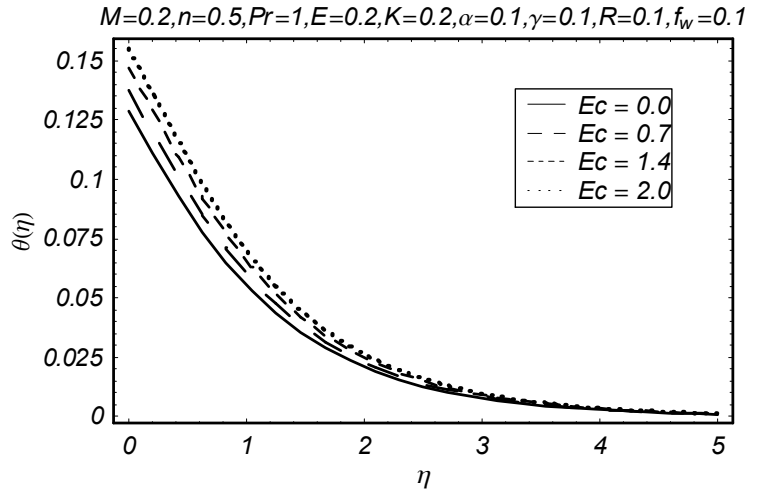

Fig. 3.13: Effect of Ec on θ.

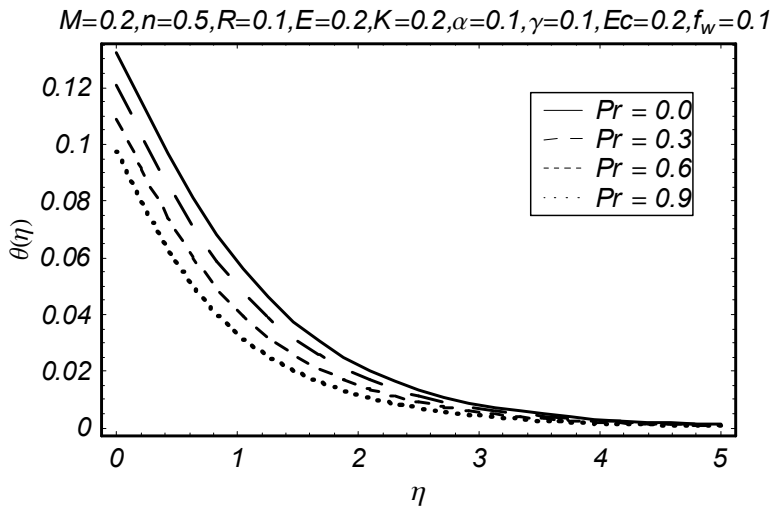

Fig. 3.14: Effect of Pr on θ.

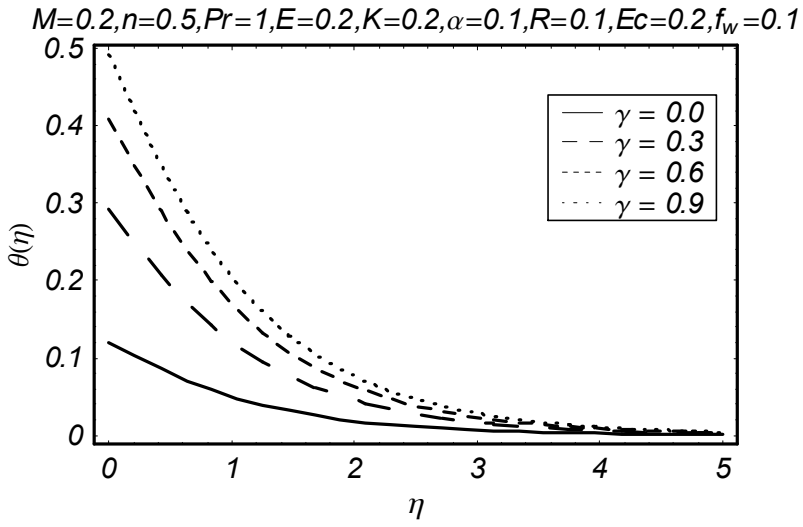

Fig. 3.15: Effect of γ on θ.

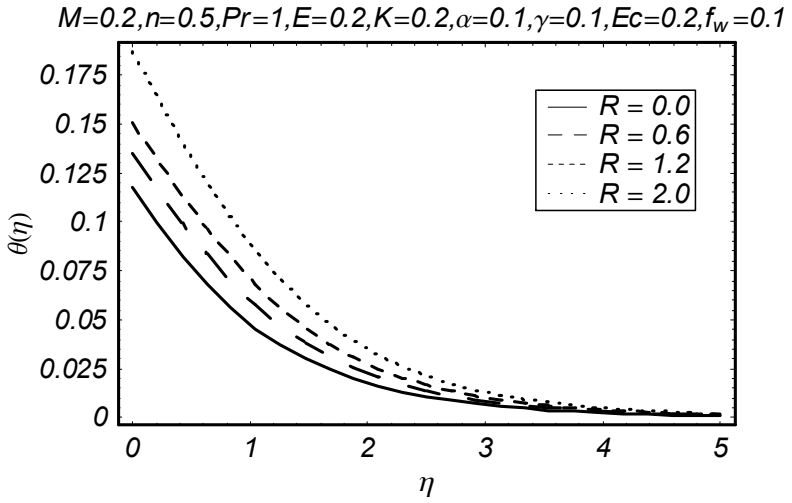

Fig. 3.16: Effect of R on θ.

Table 3.2: Values of local Nusselt number $-\theta'(0)$ for different values of the parameters when $n = 0.5$.

K	M	R	E	α	γ	β	S	Pr	$-\theta'(0)$
0.3	0.2	0.1	0.2	0.1	0.1	0.2	0.1	1.0	0.08591
0.6									0.08601
0.9									0.08608
0.2	0.3								0.08595
	0.6								0.08490
	0.9								0.08381
	0.2	0.3							0.08540
		0.6							0.08440
		0.9							0.08351
		0.1	0.3						0.08580
			0.6						0.08605
			0.9						0.08599
			0.2	0.3					0.08515
				0.6					0.08440
				0.9					0.083390
				0.1	0.3				0.2021
					0.6				0.3440
					0.9				0.3666
					0.1	0.3			0.08544
						0.6			0.08455
						0.9			0.08355
						0.2	0.3		0.08745
							0.6		0.08951
							0.9		0.09110
							0.1	2.0	0.08951
								3.0	0.09194
								4.0	0.09340

Chapter 4

Bioconvective MHD Micropolar nanofluid flow with nonlinear thermal radiation and Joule heating effects in a stratified medium

4.1 Mathematical analysis

Let us assume a two-dimensional, an incompressible MHD micro-polar nanofluid flow along a preamble stretched plane having slip velocity. The behavior of flow along with the convective transfer of heat has been examined by the uniform electric and magnetic fields. Under the boundary layer approximations, following are the governing equations:

$$\frac{\partial u}{\partial x}+\frac{\partial v}{\partial y}=0, \tag{4.1}$$

$$u\frac{\partial u}{\partial x}+v\frac{\partial u}{\partial y}=\left(\frac{\mu+k}{\rho}\right)\frac{\partial^2 u}{\partial y^2}+\frac{k}{\rho}\frac{\partial N}{\partial y}+\frac{\sigma}{\rho}\left(E_0B_0-B_0^2u\right), \tag{4.2}$$

$$u\frac{\partial N}{\partial x}+v\frac{\partial N}{\partial y}=\frac{\gamma^*}{\rho_j}\frac{\partial^2 N}{\partial y^2}-\frac{k}{\rho_j}\left(2N+\frac{\partial u}{\partial y}\right), \tag{4.3}$$

$$u\frac{\partial T}{\partial x}+v\frac{\partial T}{\partial y}=\alpha\frac{\partial^2 T}{\partial y^2}+\tau D_B\frac{\partial T}{\partial y}\frac{\partial C}{\partial y}+\tau\frac{D_T}{T_\infty}\left(\frac{\partial T}{\partial y}\right)^2+\frac{(uB_0-E_0)^2\sigma}{\rho c_p}-\frac{1}{(\rho c)_f}\frac{\partial q_r}{\partial y}, \tag{4.4}$$

$$u\frac{\partial C}{\partial x}+v\frac{\partial C}{\partial y}=\left[D_B\left(\frac{\partial^2 C}{\partial y^2}\right)+\frac{D_T}{T_\infty}\left(\frac{\partial^2 T}{\partial y^2}\right)\right], \tag{4.5}$$

$$u\frac{\partial n}{\partial x}+v\frac{\partial n}{\partial y}+\frac{bW_c}{(C_f-C_0)}\left[\frac{\partial}{\partial y}\left(n\frac{\partial C}{\partial y}\right)\right]=D_m\left(\frac{\partial^2 n}{\partial y^2}\right). \tag{4.6}$$

with suitable boundary conditions

$$u=ax+\alpha^*\left[(\mu+k)\frac{\partial u}{\partial y}+kN\right],\quad v=v_w,$$

$$N=-n\frac{\partial u}{\partial y},\quad T=T_f=T_0+b_1x,$$

$$C=C_f=C_0+d_1x,\quad n=n_f=n_0+e_1x\ \text{ at }\ y=0,$$

$$T=T_\infty=T_0+b_2x,\quad C=C_\infty=C_0+d_2x,$$

$$n=n_\infty=n_0+e_2x\qquad\text{at}\quad y=\infty,$$

$$u\to 0,\ N\to 0,\qquad\text{at}\quad y\to\infty. \tag{4.7}$$

Dimensionless form of above mathematical model is obtained by utilizing following transformations:

$$\eta=\sqrt{\frac{a}{\nu}}y,\ \psi=\sqrt{a\nu}xf(\eta),\ N=ax\sqrt{\frac{a}{\nu}}g(\eta),\ \phi(\eta)=\frac{C-C_\infty}{C_f-C_0},$$

$$\xi(\eta)=\frac{n-n_\infty}{n_f-n_0},\quad\theta(\eta)=\frac{T-T_\infty}{T_f-T_0},$$

$$u=xaf'(\eta),\ v=-\sqrt{av}f(\eta),$$

$$q_r=\frac{-4\sigma^*}{3k^*}\frac{\partial T^4}{\partial y}=\frac{-16\sigma^*}{3k^*}T^3\frac{\partial T}{\partial y},$$

$$T=T_\infty\left[1+(\theta_w-1)\theta\right]. \tag{4.8}$$

Here, satisfaction of Eq. (4.1) is inevitable. However, Eqs. $(4.2-4.7)$ take the form

$$(1+K)f'''+ff''-f'^2+Kg'-M^2f'+M^2E=0, \tag{4.9}$$

$$\left(1+\frac{K}{2}\right)g^{''}+fg^{'}-f^{'}g-K\left(2g+f^{''}\right)=0, \tag{4.10}$$

$$\left(1+\frac{4}{3}R\left(1+\left(\theta_w-1\right)\theta\right)^3\right)\theta''+4R\left(\left(\theta_w-1\right)\left(1+\left(\theta_w-1\right)\theta\right)^2\right)\theta'^2$$

$$+\Pr\left(\theta'\phi'Nb+\theta'^2Nt+f\theta'-f'\left(S+\theta\right)\right)+M^2[f'^2+E^2-2Ef']=0, \tag{4.11}$$

$$\phi^{''}+Le\Pr\left(f\phi^{'}-f'\phi\right)-\Pr LePf'+\frac{Nt}{Nb}\theta''=0, \tag{4.12}$$

$$\xi^{''}+Lb\left(f\xi^{'}-f'\xi\right)-LbQf'-Pe\left[\phi^{''}\left(\xi+\Omega\right)+\phi^{'}\xi^{'}\right]=0. \tag{4.13}$$

$$f=f_w,\ f'=1+\alpha\left(1+K\right)f'',\ g=-nf'',\ \theta=1-S,$$

$$\phi=1-P,\quad n=1-Q,\quad \text{at}\quad \eta=0$$

$$f'=0,\quad g=0,\quad \theta=0,\quad \phi=0,\quad n=0\quad \text{at } \eta=\infty \tag{4.14}$$

with

$$Lb=\frac{\nu}{D_m},\ Le=\frac{\alpha}{D_B},\ Pe=\frac{bW_c}{D_m},\ \Omega=\frac{n_\infty}{n_f-n_0},\ S=\frac{b_2}{b_1},\ \alpha_1=\frac{k_1}{(\rho c)_f} \tag{4.15}$$

$$\Pr=\frac{\nu}{\alpha},\ E=\frac{E_0}{u_wB_0},\ K=\frac{k}{\mu},\ M_1^2=M=\frac{\sigma B_0^2}{\rho a},\ P=\frac{d_2}{d_1},\ Q=\frac{e_2}{e_1}, \tag{4.16}$$

$$Nt=\frac{\tau D_T\left(T_f-T_0\right)}{\nu T_\infty},\ Nb=\frac{\tau D_B\left(C_f-C_0\right)}{\nu},\quad R=\frac{4\sigma^*T_\infty^3}{k_1k^*}. \tag{4.17}$$

Skin friction, local Nusselt, local Sherwood number and local density of number of the motile microorganisms are given by:

$$C_{f_x}=\frac{2\tau_w}{\rho\left(ax\right)^2},\ Nu_x=\frac{xq_w}{k_4(T_f-T_0)},\ Sh_x=\frac{xq_m}{D_B(C_f-C_0)},\ Nn_x=\frac{xq_n}{D_n\left(n_f-n_0\right)} \tag{4.18}$$

where

$$\tau_w=\left(\left(\mu+k\right)\frac{\partial u}{\partial y}+kN\right)_{y=0},\ q_w=-k_6\left(\frac{\partial T}{\partial y}\right)_{y=0},\ q_m=-D_B\left(\frac{\partial\phi}{\partial y}\right)_{y=0},$$

$$q_n = -D_n \left(\frac{\partial \xi}{\partial y} \right)_{y=0}. \tag{4.19}$$

Dimensionless forms of Skin friction, local Nusselt, local Sherwood number and local density of number of the motile microorganisms are appended as follows:

$$\frac{1}{2} C_{f_x} \operatorname{Re}_x^{1/2} = (1 + (1-n) K) f''(0),$$

$$Nu_x \operatorname{Re}_x^{-1/2} = -\theta'(0), \; Sh_x \operatorname{Re}_x^{-1/2} = -\phi'(0), \; Nn_x \operatorname{Re}_x^{-1/2} = -\xi'(0). \tag{4.20}$$

where $\operatorname{Re}_x = u_0 x^2 / l\nu$ is the Reynolds number.

4.2 Series solutions

Homotopy analysis method is a powerful analytical technique proposed by Liao in 1992, is engaged to find out convergent series solution. This technique has an edge over other analytical methods because of following characteristics:

i) Independency from selection of large and small parameters.

ii) Convergence of series solution is guaranteed.

iii) Ample liberty for selection of linear operators and base functions.

Following this method, the initial guesses $(f_0, g_0, \; \theta_0, \phi_0, \; \xi_0)$ and linear operators $(\mathcal{L}_f, \mathcal{L}_g, \; \mathcal{L}_\theta, \mathcal{L}_\phi, \mathcal{L}_\xi)$ are selected are given as follows:

$$f_0(\eta) = f_w + \frac{1}{1+\alpha(1+K)} (1 - \exp(-\eta)), \; g_0(\eta) = \frac{n}{1+\alpha(1+K)} \exp(-\eta),$$

$$\theta_0(\eta) = (1-S)\exp(-\eta), \quad \phi_0(\eta) = (1-P)\exp(-\eta), \quad \xi_0(\eta) = (1-Q)\exp(-\eta) \tag{4.21}$$

$$\mathcal{L}_f = f''' - f', \; \mathcal{L}_g = g'' - g, \quad \mathcal{L}_\theta = \theta'' - \theta,$$

$$\mathcal{L}_\phi = \phi'' - \phi, \quad \mathcal{L}_\xi = \xi'' - \xi \tag{4.22}$$

with

$$\mathcal{L}_f (H_1 + H_2 \exp(-\eta) + H_3 \exp(\eta)) = 0, \tag{4.23}$$

$$\mathcal{L}_g (H_4 \exp(-\eta) + H_5 \exp(\eta)) = 0, \tag{4.24}$$

$$\mathcal{L}_\theta \left(H_6 \exp(-\eta) + H_7 \exp(\eta)\right) = 0, \tag{4.25}$$

$$\mathcal{L}_\phi \left(H_8 \exp(-\eta) + H_9 \exp(\eta)\right) = 0, \tag{4.26}$$

$$\mathcal{L}_\xi \left(H_{10} \exp(-\eta) + H_{11} \exp(\eta)\right) = 0 \tag{4.27}$$

where H_i $(i = 1 - 11)$ are the arbitrary constants.

4.3 Convergence analysis

Homotopy analysis technique is used for the series solutions of highly nonlinear problems. Therefore, we have plotted the $\hbar$-curves in the Figure 4.1. The admissible ranges of the auxiliary parameters $\hbar_f$, $h_g, \hbar_\theta, h_\xi$ and $\hbar_\phi$ are $-1.4 \leq \hbar_f \leq -0.1$, $-1.2 \leq \hbar_g \leq -0.1, -1.2 \leq \hbar_\theta \leq -0.1, -1.2 \leq \hbar_\phi \leq -0.1$ and $-1.2 \leq \hbar_\xi \leq -0.1$ when $Nt = Nb = 2.0$, $\Omega = 0.2$, $Pe = \alpha = 0.5$, $R = 0.1$, $S = \delta = 0.4$, Pr $= 1.2$, $Lb = Le = 1.0$, $\theta_w = 1.01$ and $M = E = 0.7$. Table 4.1 expresses the convergence of series solutions of momentum, micro-rotation, energy equation, concentration and bio-convection and it demonstrates that the 25^{th} order of guesstimates are adequate for the convergent series solution that are in good agreement to graphical illustration shown in figure 4.1.

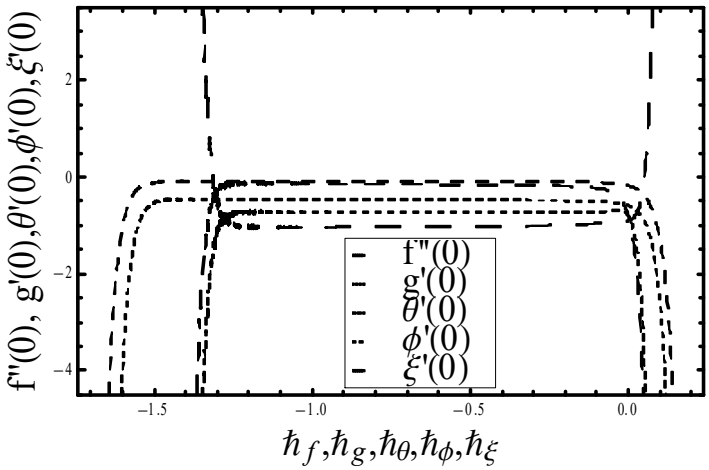

Fig. 4.1: $\hbar-$curves of f', g, θ, ϕ and ξ.

Table 4.1: Convergence of series solution for different order of approximations when $Nt = Nb = 2.0$, $\Omega = 0.2$, $Pe = \alpha = 0.5$, $R = 0.1$, $S = \delta = 0.4$, Pr $= 1.2$, $Lb = Le = 1.0$, $\theta_w = 1.01$

and $M = E = 0.7$, $\hbar_f = \hbar_g = \hbar_\theta = \hbar_\phi = \hbar_\xi = -0.8$.

Order of approximations	$-f''(0)$	$-g'(0)$	$-\theta'(0)$	$-\phi'(0)$	$-\xi'(0)$
1	0.52582	0.13145	0.22653	0.56282	0.94438
5	0.49505	0.10587	0.20271	0.73186	0.97843
10	0.48358	0.10058	0.17451	0.73428	1.00280
15	0.47771	0.09892	0.16275	0.73357	1.01560
20	0.47391	0.09822	0.15635	0.73234	1.02410
25	0.47114	0.09789	0.15240	0.73086	1.03000
30	0.47114	0.09789	0.15240	0.73086	1.03000

4.4 Results and discussion

This section is devoted to observe the effects of numerous parameters on associated profiles. Higher values of the slip parameter α reduce the velocity field and corresponding boundary thickness as depicted in figure 4.2. In fact higher velocity slip parameter results in less adhesive force between the wall and fluid particles which provides more resistance for transfer of stretching velocity to the fluid. Therefore velocity distribution decreases. From figure 4.3 we observed that velocity field and its connected boundary layer thickness are decreasing functions of material parameter K. It is analyzed that velocity distribution is higher at the surface of wall for small values of material parameter K. Explanation of an electric field E on the velocity distribution is represented in figure 4.4. It is perceived that velocity and associated velocity boundary layer thickness has foremost behavior for advanced values of an electric parameter. It is because of fact that addition in an electric field resembles to a higher Lorentz force in the path of flow. Therefore, velocity distribution rises. The behavior of suction parameter f_w on the velocity distribution is showed in figure 4.5. Velocity distribution is foremost for small quantities of suction parameter. Additional velocity boundary layer thickness turns out to be more thin with an increment in suction parameter. Figure 4.6 is drawn to understand the influence of Hartmann number M on velocity field. A reduction in velocity profile is detected with a gradual increase in the values on M. This is because of increasing values of the Hartmann number augments the Lorentz force that resist the fluid motion and effects in diminution in the

velocity distribution. Furthermore, momentum boundary layer thickness also decrease. Figure 4.7 is outlined for behavior of the Hartmann number M on micro-rotation. The micro-rotation is found to increase when the Hartmann number increases. Physically it aligns that a high magnetic field tends to rotate the fluid elements more obviously which offers more confrontation in the horizontal velocity although an increase in micro-rotation velocity. Consequence of an electric field parameter E on micro-rotation is presented in figure 4.8. It is perceived that micro-rotation field decreases when electric field is increased. Analysis of material parameter K on micro-rotation velocity is demonstrated in figure 4.9. Micro-rotation distribution decreases when material parameter K increases. Figure 4.10 is shown to perceive the influence of slip parameter α on micro-rotation distribution. It is observed that micro-rotation declines by intensifying slip parameter. Figure 4.11 is depicted to see the influence of Prandtl number Pr on temperature distribution. It is noted that an energy profile is reducing function of Pr. This is since an increase in the Prandtl number produces a feebler thermal diffusivity and thinner boundary layer thickness. In figures 4.12 and 4.13 it is noted that the temperature of fluid and thermal boundary layer thickness are growing function of Nb and Nt, because to that the concentration profile rises. Clearly when Nt rises then extra nanoparticles transfer from the heated surface that ultimately rises the concentration of nano-particles. Both temperature field and its thermal boundary layer thickness increases with the mounting values of radiation parameter R. That fact is exposed in figure 4.14. Figure 4.15 displays the influence of thermal stratification parameter S on temperature profile. It is observed that thermal boundary layer increases for small S . In fact when S increases then temperature difference between heated surface and away from the surface decreases. Thus fluid temperature is observed to decrease. The influence of Lewis number Le on concentration distribution is drawn in figure 4.16. It is seen that concentration profile declines with the rise in values of Le. As an increase in Le is proportional to thinner concentration boundary layer and weaker mass diffusivity. Figures 4.17 and 4.18 shows the result of thermophoresis parameter Nt and Brownian motion parameter Nb on concentration distribution. An opposite behavior on concentration field is observed for Nb and Nt, i.e., the mass transfer decrease for increasing Nb and improve for rising values of Nt. Influence of concentration stratification parameter P on concentration profile is displayed in figure 4.19. It is analyzed that the volumetric fraction between surface and reference nanopar-

ticles decrease when P increases. Hence the concentration profile decreases. Influence of motile density stratification parameter Q on density profile is sketched in figure 4.20. An increase in Q decreases the concentration difference of microorganisms between the surface and away from the surface and so decrease in the density profile is noticed. Variation of Peclet number Pe on motile density profile is presented in figure 4.22. It is noted that the motile density profile decreases for a larger Pe. Increase in Pe affects to a decrease in the diffusivity of microorganisms and hence motile density of fluid declines. Figures 4.21 and 4.23 highlighted out the influence of microorganism's intensity difference parameter and bio-convection Lewis number Lb on motile density. It is observed that rise in Ω improves the concentration of microorganisms in the ambient fluid and reduces in the density profile. Though for higher values of Lb the diffusivity of microorganisms declines and therefore the motile density decays. Influences of E and M on the Skin friction number is shown in figure 4.24. It is disclosed that the Skin friction number increases for increasing values of E and M . Influences of Nt and Nb on the local Nusselt number is shown in figure 4.25. It is disclosed that the local Nusselt number increases for increasing values of Nt and Nb. Influences of Le and Nt on the local Sherwood number is shown in figure 4.26. It is disclosed that the local Sherwood number decreases for increasing values of Le and Nt . Influences of Pe and Lb on the local density number is shown in figure 4.27. It is disclosed that the local density number increases for increasing values of Pe and Lb .

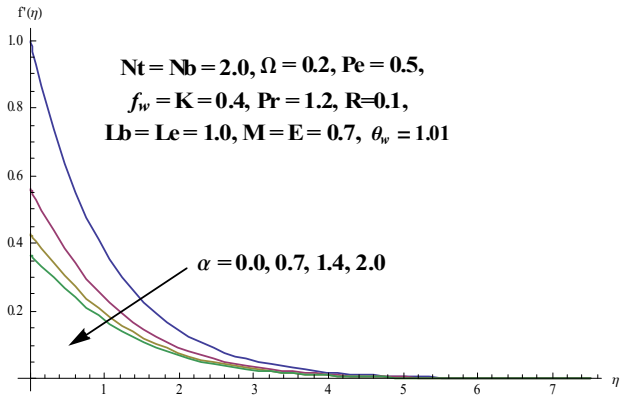

Fig. 4.2: Effect of α on f'.

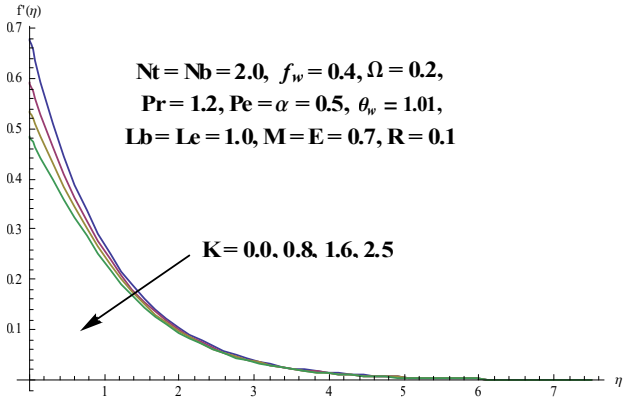

Fig. 4.3: Effect of K on f'.

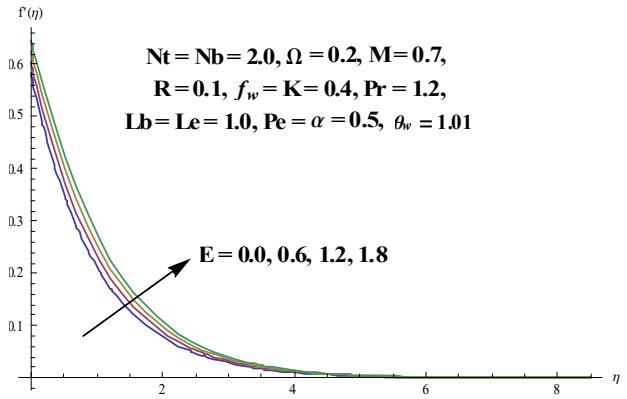

Fig. 4.4: Effect of E on f'.

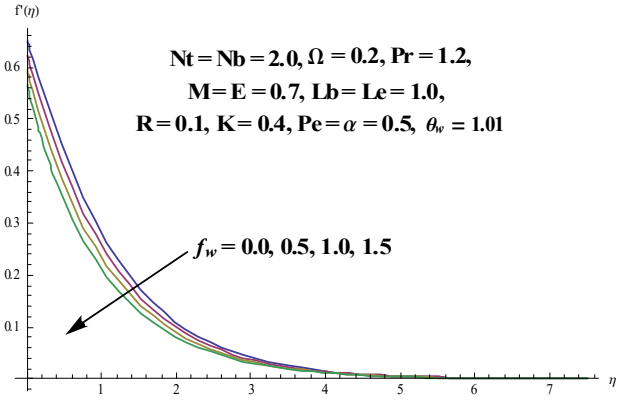

Fig. 4.5: Effect of f_w on f'.

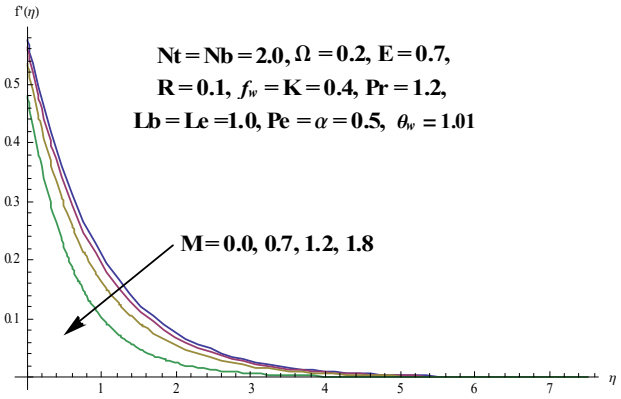

Fig. 4.6: Effect of M on f'.

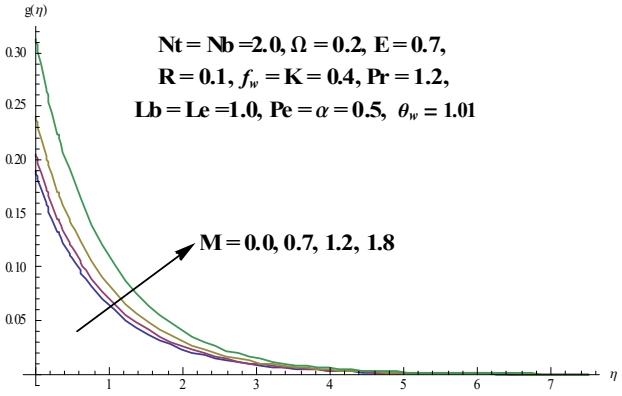

Fig. 4.7: Effect of M on g.

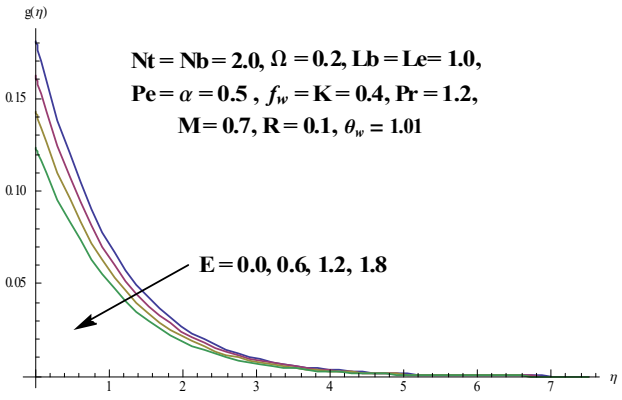

Fig. 4.8: Effect of E on g.

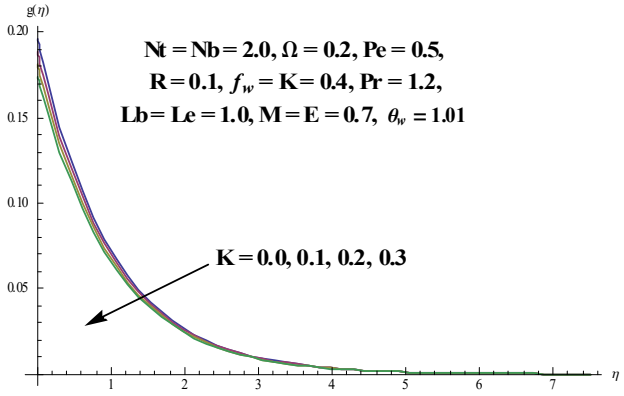

Fig. 4.9: Effect of K on g.

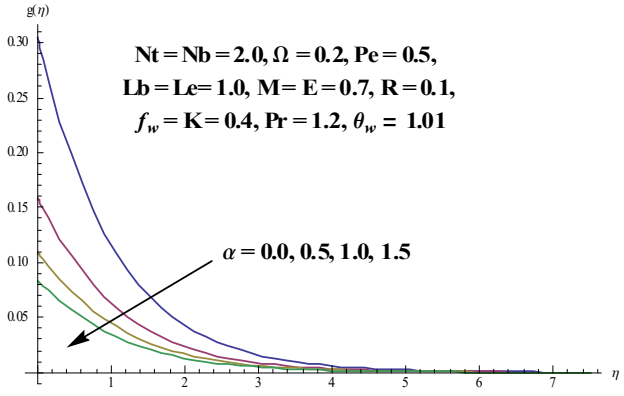

Fig. 4.10: Effect of α on g.

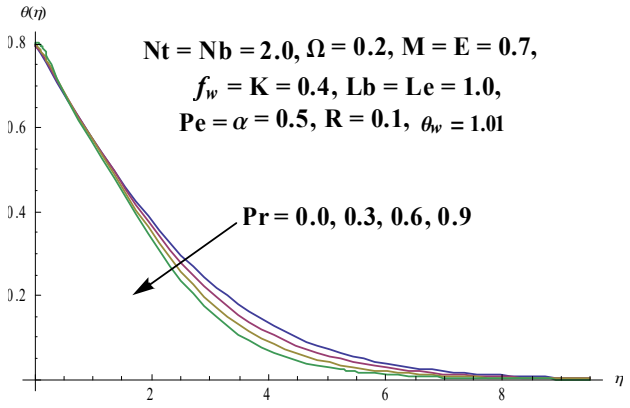

Fig. 4.11: Effect of Pr on θ.

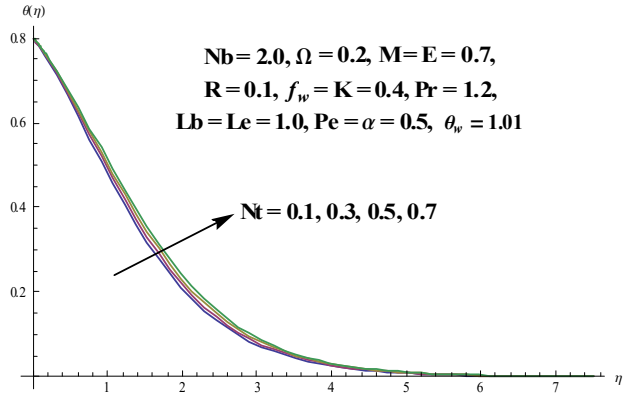

Fig. 4.12: Effect of Nt on θ.

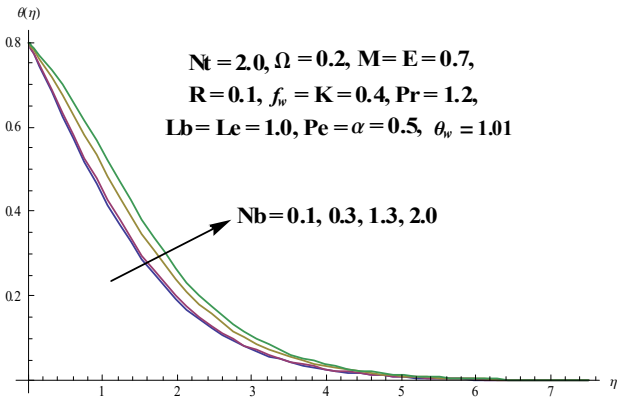

Fig. 4.13: Effect of Nb on θ.

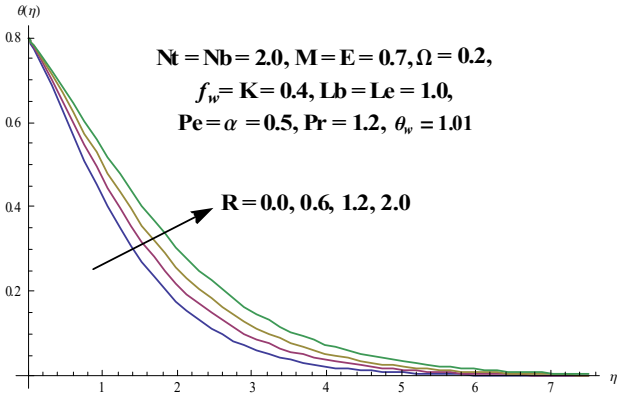

Fig. 4.14: Effect of R on θ.

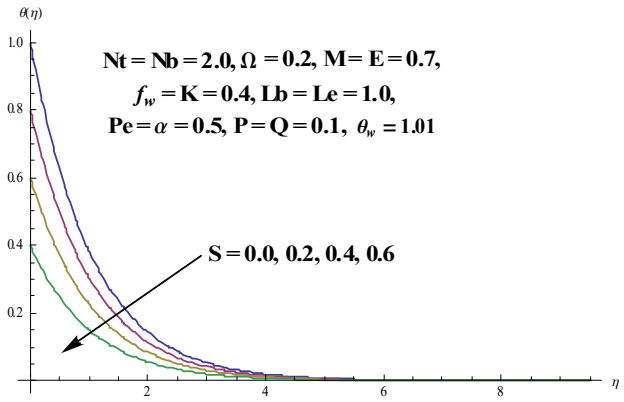

Fig. 4.15: Effect of S on θ.

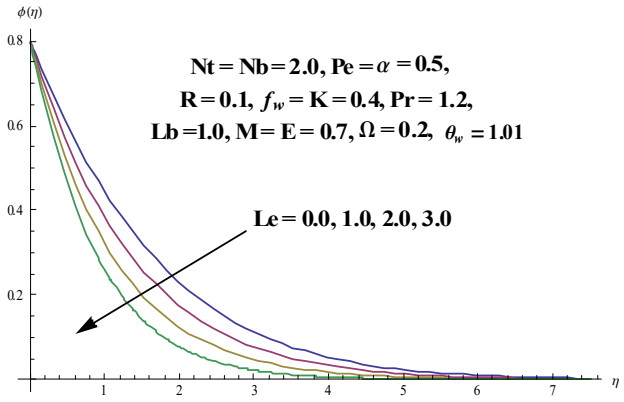

Fig. 4.16: Effect of Le on ϕ.

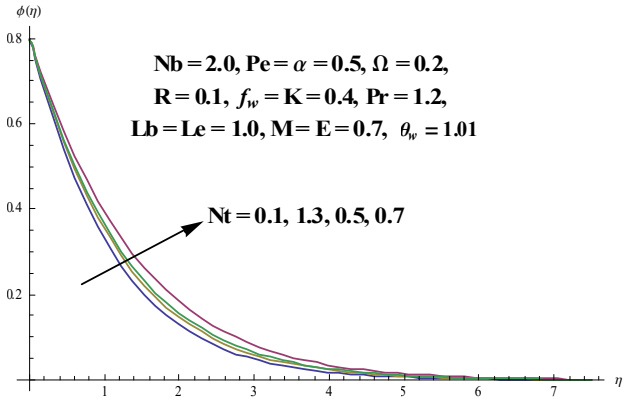

Fig. 4.17: Effect of Nt on ϕ.

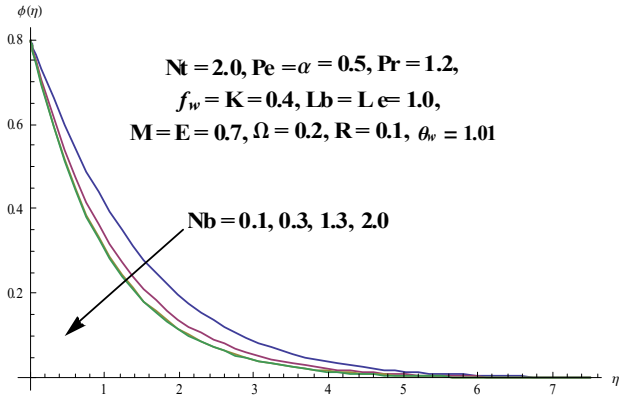

Fig. 4.18: Effect of Nb on ϕ.

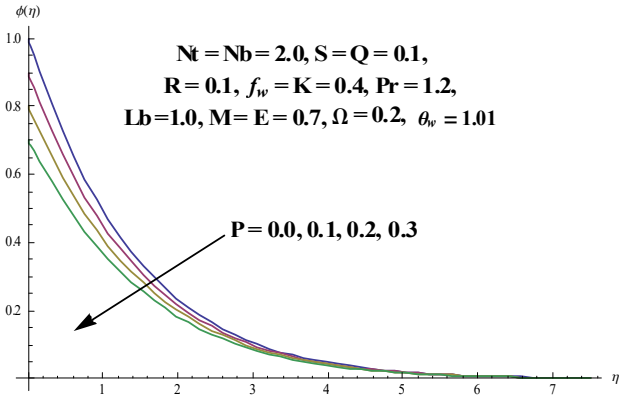

Fig. 4.19: Effect of P on ϕ.

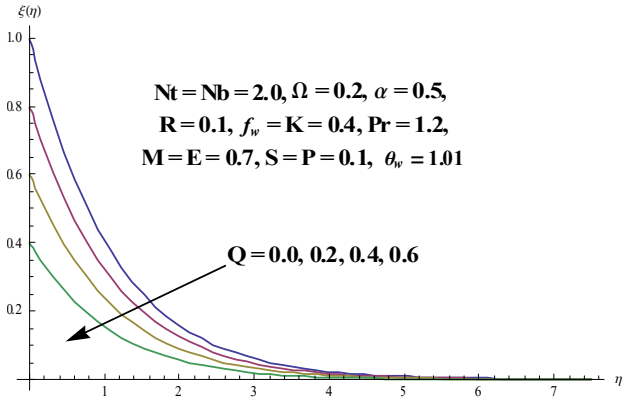

Fig. 4.20: Effect of Q on ξ.

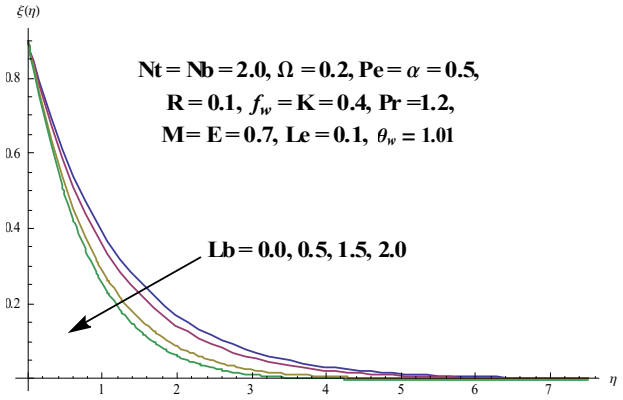

Fig. 4.21: Effect of Lb on ξ.

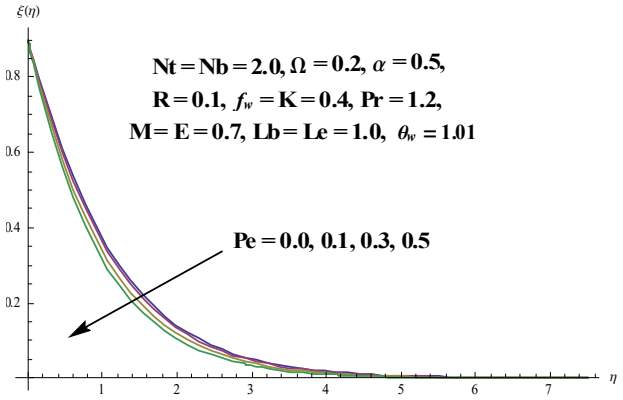

Fig. 4.22: Effect of Pe on ξ.

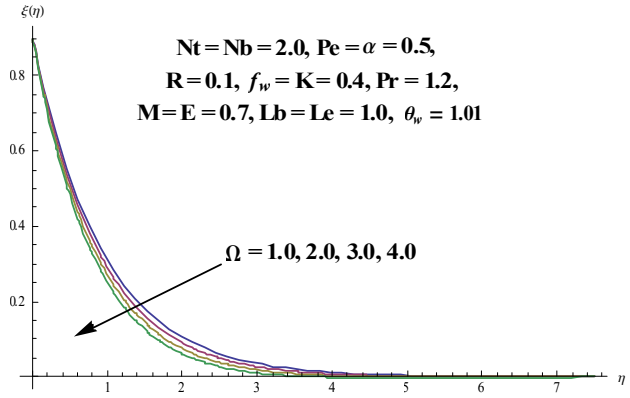

Fig. 4.23: Effect of Ω on ξ.

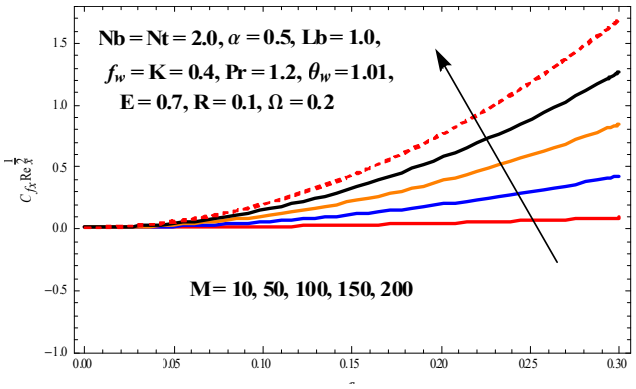

Fig. 4.24: Effect of E and M on $C_{f_x}\,\mathrm{Re}_x^{1/2}$.

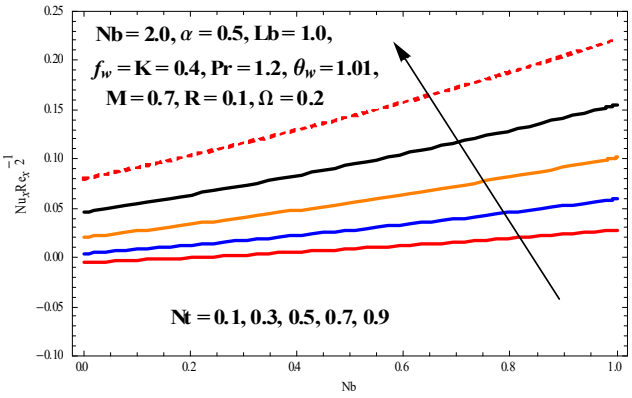

Fig. 4.25: Effect of Nb and Nt on $Nu_x \, \mathrm{Re}_x^{-1/2}$.

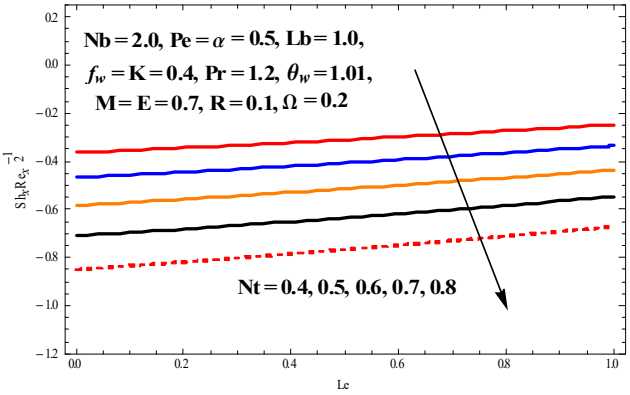

Fig. 4.26: Effect of Le and Nt on $Sh_x \, \mathrm{Re}_x^{-1/2}$.

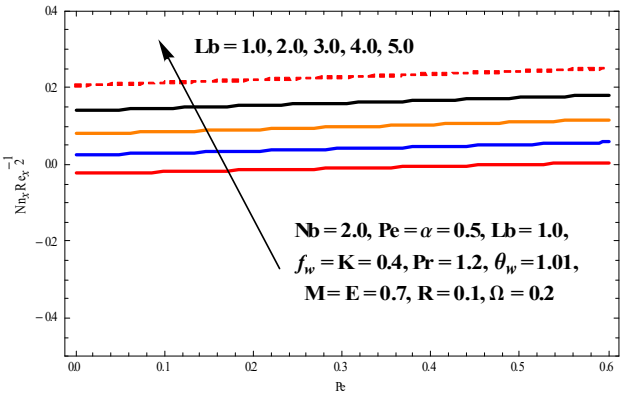

Fig. 4.27: Effect of Pe and Lb on $Nn_x \operatorname{Re}_x^{-1/2}$.

Chapter 5

Conclusions and Future work

5.1 Chapter 3

Here, we have examined the MHD boundary layer flow of micropolar fluid with slip velocity and electric field. Convective heat transfer analysis is carried out with Joule heating and thermal radiation effects. The main observations are:

- Material parameter decreases the velocity and micro-rotation profiles.
- Velocity and micro-rotation profiles decrease with an increase in slip parameter.
- Electric field increases the temperature and thermal boundary layer thickness.
- Velocity profile decreases with an increase in Hartmann number while the temperature increases.
- Biot number and radiation parameter increase both the temperature and thermal boundary layer thickness.

5.2 Chapter 4

Here, we have examined the MHD micropolar nanofluid with stratified medium. Bioconvective heat transfer analysis is carried out with Joule heating and non thermal radiation effects. The main observations are:

- Material parameter decreases the velocity and micro-rotation profiles.
- Velocity and micro-rotation profiles decrease with an increase in slip parameter.
- Electric field increases the temperature and thermal boundary layer thickness.
- Velocity profile decreases with an increase in Hartmann number while the temperature increases.
- Thermophoresis parameter and Brownian motion parameter increase while the temperature increase.

5.3 Future work

Few interesting possible problems that could be researched in future are as follows:

- The work may be extended to any non-Newtonian fluid.
- The impact of Darcy-Forchheimer may also be added.
- The effects of heat generation/absorption, with Joule heating and viscous dissipation may also be entertained.
- The concentration equation may be enriched by addition of chemical reaction or Arrhenis activation energy with gravity effects.
- The boundary conditions may be changed melting heat, convective heat and mass conditions.

Bibliography

[1] A. Eringen, "Theory of Micropolar Fluids," J. Math. Mech., vol. 16, no. 1, pp. 1–18, 1966.

[2] R. Nazar, N. Amin, D. Filip, and I. Pop, "Stagnation point flow of a micropolar fluid towards a stretching sheet," Int. J. Non. Linear. Mech., vol. 39, no. 7, pp. 1227–1235, 2004.

[3] D. Pal and S. Chatterjee, "Heat and mass transfer in MHD non-Darcian flow of a micropolar fluid over a stretching sheet embedded in a porous media with non-uniform heat source and thermal radiation," Commun. Nonlinear Sci. Numer. Simul., vol. 15, no. 7, pp. 1843–1857, 2010.

[4] F. Mabood, W. A. Khan, and A. I. M. Ismail, "MHD stagnation point flow and heat transfer impinging on stretching sheet with chemical reaction and transpiration," Chem. Eng. J., vol. 273, pp. 430–437, 2015.

[5] S. Nadeem, M. Y. Malik, and N. Abbas, "Heat transfer of three dimensional micropolar fluids on Riga plate.," Can. J. Phys., pp. 1–22, 2019.

[6] M. Ramzan, M. Farooq, T. Hayat, and J. D. Chung, "Radiative and Joule heating effects in the MHD flow of a micropolar fluid with partial slip and convective boundary condition," J. Mol. Liq., 2016.

[7] S. S. Ghadikolaei, K. Hosseinzadeh, M. Hatami, and D. D. Ganji, "MHD boundary layer analysis for micropolar dusty fluid containing Hybrid nanoparticles (Cu■Al2O3) over a porous medium," J. Mol. Liq., 2018.

[8] J. Sui, P. Zhao, Z. Cheng, and M. Doi, "Influence of particulate thermophoresis on convection heat and mass transfer in a slip flow of a viscoelasticity-based micropolar fluid," Int. J. Heat Mass Transf., 2018.

[9] O. K. Koriko, I. L. Animasaun, A. J. Omowaye, and T. Oreyeni, "The combined influence of nonlinear thermal radiation and thermal stratification on the dynamics of micropolar fluid along a vertical surface," Multidiscip. Model. Mater. Struct., 2019.

[10] D. Yadav, C. Kim, J. Lee, and H. H. Cho, "Influence of magnetic field on the onset of nanofluid convection induced by purely internal heating," Comput. Fluids, 2015.

[11] M. Farooq, M. I. Khan, M. Waqas, T. Hayat, A. Alsaedi, and M. I. Khan, "MHD stagnation point flow of viscoelastic nanofluid with non-linear radiation effects," J. Mol. Liq., 2016.

[12] M. Sheikholeslami, M. M. Rashidi, T. Hayat, and D. D. Ganji, "Free convection of magnetic nanofluid considering MFD viscosity effect," J. Mol. Liq., vol. 218, pp. 393–399, 2016.

[13] M. Sheikholeslami, "Numerical simulation of magnetic nanofluid natural convection in porous media," Phys. Lett. Sect. A Gen. At. Solid State Phys., vol. 381, no. 5, pp. 494–503, 2017.

[14] A. Pramuanjaroenkij, A. Tongkratoke, and S. Kakaç, "Numerical Study of Mixing Thermal Conductivity Models for Nanofluid Heat Transfer Enhancement," J. Eng. Phys. Thermophys., vol. 91, no. 1, pp. 104–114, 2018.

[15] D. Lu, M. Ramzan, S. Ahmad, J. D. Chung, and U. Farooq, "A numerical treatment of MHD radiative flow of Micropolar nanofluid with homogeneous-heterogeneous reactions past a nonlinear stretched surface," Sci. Rep., 2018.

[16] S. Nadeem, M. N. Khan, N. Muhammad, and S. Ahmad, "Mathematical analysis of bioconvective micropolar nanofluid," Journal of Computational Design and Engineering, 2018.

[17] N. Abbas, S. Saleem, S. Nadeem, A. A. Alderremy, and A. U. Khan, "On stagnation point flow of a micro polar nanofluid past a circular cylinder with velocity and thermal slip," Results Phys., vol. 9, no. March, pp. 1224–1232, 2018.

[18] M. Sheikholeslami, M. B. Gerdroodbary, R. Moradi, A. Shafee, and Z. Li, "Application of Neural Network for estimation of heat transfer treatment of Al[Formula presented]O[Formula presented]-H[Formula presented]O nanofluid through a channel," Comput. Methods Appl. Mech. Eng., 2019.

[19] Z. Shah, S. Islam, T. Gul, E. Bonyah, and M. Altaf Khan, "The electrical MHD and Hall current impact on micropolar nanofluid flow between rotating parallel plates," Results Phys., vol. 9, pp. 1201–1214, 2018.

[20] A. Khan, Z. Shah, S. Islam, S. Khan, W. Khan, and A. Z. Khan, "Darcy–Forchheimer flow of micropolar nanofluid between two plates in the rotating frame with non-uniform heat generation/absorption," Adv. Mech. Eng., vol. 10, no. 10, pp. 1–16, 2018.

[21] M. A. Sadiq, A. U. Khan, S. Saleem, and S. Nadeem, "Numerical simulation of oscillatory oblique stagnation point flow of a magneto micropolar nanofluid," RSC Adv., vol. 9, no. 9, pp. 4751–4764, 2019.

[22] I. Ullah, S. Shafie, O. D. Makinde, and I. Khan, "Unsteady MHD Falkner-Skan flow of Casson nanofluid with generative/destructive chemical reaction," Chem. Eng. Sci., vol. 172, pp. 694–706, 2017.

[23] I. Ullah, S. Shafie, I. Khan, and K. L. Hsiao, "Brownian diffusion and thermophoresis mechanisms in Casson fluid over a moving wedge," Results Phys., 2018.

[24] S. Rashidi, M. Eskandarian, O. Mahian, and S. Poncet, "Combination of nanofluid and inserts for heat transfer enhancement: Gaps and challenges," J. Therm. Anal. Calorim., 2019.

[25] M. Sheikholeslami, "CuO-water nanofluid flow due to magnetic field inside a porous media considering Brownian motion," J. Mol. Liq., 2018.

[26] T. Hussain, S. A. Shehzad, A. Alsaedi, T. Hayat, and M. Ramzan, "Flow of Casson nanofluid with viscous dissipation and convective conditions: A mathematical model," J. Cent. South Univ., vol. 22, no. 1132–1140, 2015.

[27] T. Hayat, Z. Abbas, I. Pop, and S. Asghar, "Effects of radiation and magnetic field on the mixed convection stagnation-point flow over a vertical stretching sheet in a porous medium," Int. J. Heat Mass Transf., vol. 53, no. 1–3, pp. 466–474, 2010.

[28] D. Pal and B. Talukdar, "Buoyancy and chemical reaction effects on MHD mixed convection heat and mass transfer in a porous medium with thermal radiation and Ohmic heating," Commun. Nonlinear Sci. Numer. Simul., 2010.

[29] K. Bhattacharyya and G. C. Layek, "Effects of suction/blowing on steady boundary layer stagnation-point flow and heat transfer towards a shrinking sheet with thermal radiation," Int. J. Heat Mass Transf., 2011.

[30] T. Hussain, S. A. Shehzad, T. Hayat, A. Alsaedi, F. Al-Solamy, and M. Ramzan, "Radiative hydromagnetic flow of Jeffrey nanofluid by an exponentially stretching sheet," PLoS One, 2014.

[31] M. Ramzan and M. Bilal, "Time dependent MHD nano-second grade fluid flow induced by permeable vertical sheet with mixed convection and thermal radiation," PLoS One, 2015.

[32] T. Hayat, T. Muhammad, A. Alsaedi, and M. S. Alhuthali, "Magnetohydrodynamic three-dimensional flow of viscoelastic nanofluid in the presence of nonlinear thermal radiation," J. Magn. Magn. Mater., vol. 385, pp. 222–229, 2015.

[33] M. Ramzan, M. Bilal, and J. D. Chung, "Effects of thermal and solutal stratification on jeffrey magneto-nanofluid along an inclined stretching cylinder with thermal radiation and heat generation/absorption," Int. J. Mech. Sci., 2017.

[34] D. Pal and G. Mandal, "Thermal radiation and MHD effects on boundary layer flow of micropolar nanofluid past a stretching sheet with non-uniform heat source/sink," Int. J. Mech. Sci., 2017.

[35] M. K. Siddiq, A. Rauf, S. A. Shehzad, F. M. Abbasi, and M. A. Meraj, "Thermally and solutally convective radiation in MHD stagnation point flow of micropolar nanofluid over a shrinking sheet," Alexandria Eng. J., 2018.

[36] S. S. Ghadikolaei, K. Hosseinzadeh, and D. D. Ganji, "Numerical study on magnetohydrodynic CNTs-water nanofluids as a micropolar dusty fluid influenced by non-linear thermal radiation and joule heating effect," Powder Technol., 2018.

[37] S. J. Liao, *Homotopy Analysis Method in Nonlinear Differential Equations*, Springer &Higher Education Press, Heidelberg, 2012.

[38] S. Abbasbandy, M.S. Hashemi and I. Hashim, On convergence of homotopy analysis method and its application to fractional integro-differential equations, Quaest. Math. 36 (2013) 93–105.

ORIGINALITY REPORT

1%	0%	1%	1%
SIMILARITY INDEX	INTERNET SOURCES	PUBLICATIONS	STUDENT PAPERS

PRIMARY SOURCES

1	Orhan Aydın. "Non-Darcian Forced Convection Flow of Viscous Dissipating Fluid over a Flat Plate Embedded in a Porous Medium", Transport in Porous Media, 06/2008 Publication	<1%
2	Submitted to Heriot-Watt University Student Paper	<1%
3	Submitted to King Saud University Student Paper	<1%